

DECLASSIFIED

NASA TECHNICAL MEMORANDUM



NASA TM X-52044

NASA TM X-52044

GPO PRICE \$ _____

CFSTI PRICE(S) \$ _____

Hard copy (HC) 3.00

Microfiche (MF) .50

ff 653 July 65

CLASSIFIED CHANGED
to unclassified
by John C. Landers
Ltr. 9-22-65

NUCLEAR ROCKET SIMULATOR TESTS
FLOW INITIATION WITH NO TURBINE GAS;
TANK PRESSURE, 35 PSIA; RUN 1

Lewis Research Center
Cleveland, Ohio

Special Release -
Preliminary information.
Not to be referenced.

FACILITY FORM 602

<u>N66-11627</u> (ACCESSION NUMBER)	_____ (THRU)
<u>57</u> (PAGES)	<u>1</u> (CODE)
_____ (NASA CR OR TMX OR AD NUMBER)	<u>22</u> (CATEGORY)

DECLASSIFIED

NUCLEAR ROCKET SIMULATOR TESTS

FLOW INITIATION WITH NO TURBINE GAS;

TANK PRESSURE, 35 PSIA; RUN 1

Lewis Research Center

ABSTRACT

A presentation of the overall test objectives of the Nuclear Rocket Simulator Tests along with a brief description of the research facility and data system is given. The primary objective of the first liquid-hydrogen run was to check out the operational procedure, the test setup, the instrumentation, and the data acquisition system. Some useful data were obtained. Temperature and pressure measurements taken for the first liquid-hydrogen run are presented as a function of time for selected locations and components in the system.

11627

Author



TABLE OF CONTENTS

	Page
OBJECTIVES -----	1
Overall Test Objectives -----	1
Run 1 Objectives -----	2
RESEARCH APPARATUS -----	2
DATA SYSTEM -----	3
Instrumentation -----	3
Data Acquisition -----	3
Data Processing -----	3
RESULTS AND DISCUSSION -----	4
System Performance -----	4
Component Performance -----	4
CONCLUDING REMARKS -----	5
REFERENCE -----	5
TABLE I.- INSTRUMENTATION -----	6
LIST OF FIGURES -----	12





NUCLEAR ROCKET SIMULATOR TESTS:

FLOW INITIATION WITH NO TURBINE GAS;

TANK PRESSURE, 35 PSIA; RUN 1

OBJECTIVES

Analytical attempts to predict system dynamics and component performance are being made. Difficulty in predicting accurate conditions at component interfaces and at the initiation of flow through the system leads to uncertain results. Currently, analog studies on the nuclear rocket systems begin with about 10 percent of rated flow and 1 percent of rated reactor power and as a consequence, an important phase of startup is not included. In order to obtain adequate information during this initial period, the experimental study of system dynamics and component phenomena in cold flow tests conducted in the B-1 nuclear rocket simulator (see reference 1) was initiated.

Overall Test Objectives

The ultimate objective is to be able to specify control system parameters which will insure safe programmed start-up. A detailed description of the B-1 test engine and facility is given in reference 1. The experimental program planned for B-1 will include investigation of the following major problem areas:

- Dynamics and control during startup.
- Heat transfer and flow during startup.
- Mechanical phenomena.
- Turbopump characteristics.

Specifically, the experimental objectives of the program are:

1. Determine severity of two-phase flow oscillations in the system.
2. Determine time of chilldown required to smooth out flow instabilities before bootstrapping can begin.
3. Determine turbine flow required to bootstrap.
4. Determine temperature-time variations of all components of the system: turbopump, piping, nozzle, reflector, and core.
5. Determine if choking (sonic velocity) occurs in the nozzle coolant passages.





6. Determine the state of the hydrogen throughout the system during the start transient, and in particular determine if liquid hydrogen enters the core.
7. Determine turbopump operating characteristics such as flowrate, speed, pressure drop, etc. during startup, and whether stall or cavitation occurs.
8. Determine local and gross overall hydrogen flow and density maldistributions in the nozzle, reflector, and core.
9. Determine amplitude, frequency, and direction of vibrations in the turbopump, nozzle, and reactor.
10. Obtain transient heat transfer and flow data in a large diameter pipe (between pump discharge and nozzle inlet).
11. Obtain data to verify or improve calculation methods for predicting pressure drop, fluid temperatures, and material temperatures.

Run 1 Objectives

One of the primary objectives of the first liquid hydrogen run was to check out the operational procedure, the test setup, the instrumentation, and the data acquisition system. In a facility the size of B-1, although previously operated with gaseous helium and liquid nitrogen, experience in operation with liquid hydrogen is essential; the first several runs furnished this experience. In addition to the checkout, some useful data were obtained.

RESEARCH APPARATUS

A detailed description of the B-1 facility, the test apparatus, the instrumentation, the data acquisition system, and the data processing procedure is given in reference 1. A photograph showing some details of the installation of the Mark IX turbopump apparatus is presented in figure 1(a) herein, and the second photograph showing the propellant feed line, nozzle, and reactor is presented in figure 1(b). The locations of the several motion picture and television cameras are also shown in figure 1(b). Figure 2 shows a schematic diagram of the complete cold flow experiment.



DATA SYSTEM

Instrumentation

Prior to installation, the complete research apparatus including tank, turbopump, piping, nozzle and reactor were instrumented at approximately 900 points. A complete tabulation of all measurement item numbers and installation details is given in reference 1.

The first liquid hydrogen run in the B-1 facility included the measurement of 290 items; data from nearly half of these are reported herein. Table I lists and describes each measurement and figures 2, 3, and 4 show the location of the stations used.

Data Acquisition

The various data recording instruments used are shown in Table I. A 4000 cycle sampling rate digital system with 192 inputs and a 10,000 cycle sampling rate with 100 inputs were used for these tests. For recording higher frequency information that may be present, some of the data were recorded on FM tape and on oscillographs. An estimated overall accuracy for each measurement is also included in Table I, as well as remarks regarding problems that may have occurred during the test. The accuracy estimates include possible errors in the transducer calibrations, data acquisition system, and data processing. Details of the various signal conditioning and data acquisition systems are given in reference 1.

Data Processing

The data recorded on the FM magnetic tape was retrieved through appropriate electronic equipment and recorded on a recording oscillograph. Difficulty was encountered with some channels which had 400 cycles per second noise, from an unknown source, superimposed on the data. This noise was eliminated in the data records presented herein by filtering the signals with 120 cycles per second filters.

The 10 KC digital data was processed through an 1103 computer program (see reference 1) which converted the signals to engineering units and applied the individual calibration of each transducer. The output from the computer is a tabulation of the value of each variable at each 1/10th of a second during the complete run. In addition to the tabulated values, selected variables are plotted against time on the output typewriter. Reproductions of some of these plots are presented in this report.

The processing of the 4 KC digital data includes not only the calibration and conversion to engineering units, but also calculations of interest for heat transfer and flow phenomena in the system.

The data which were recorded on direct writing oscillographs were converted to engineering units and calibrations were applied manually.

RESULTS AND DISCUSSION

System Performance

Immediately prior to starting flow in the nuclear rocket simulator, the following conditions existed in the system: The tank pressure was constant at approximately 35 psia; the ejector exhaust pressure was approximately 0.7 psia. The system was precooled down to liquid hydrogen temperature from the tank to the main valve. The pump was free to rotate but with no turbine flow. The test run began when the tank shutoff valve started opening at 10 percent of full open per second. No attempt was made to control the flow rate during the chilldown. The time history of the flow rate and the pressures in various parts of the system was therefore a result of the change in main valve area and the resistance to flow in the various components of the systems and the change in density of the fluid due to heat transfer.

The variation of flow rate with time during the run at two stations in the system is presented in figure 5. The upper curve is the flow rate measured by the turbine flowmeter which is located at the bottom of the supply tank. The lower curve is the flow rate calculated from pressure measurements at the exhaust nozzle which discharges into the ejector exhaust system. The difference between the two curves can be explained in part by storage of hydrogen in the system during the run. Other uncertainties in calibration of both flow measurements also exist. Figures 6 through 21 show plots of static pressure or fluid temperature at various interfaces in the system. The remainder of the plots deal with components only.

Component Performance

The system startup history of the Mark IX turbopump is shown in figure 22. The plot was constructed from digital data using one second time intervals to determine variations in speed, flowrate, and static pressure drop. At startup the speed indicator shows the shape of the gear tooth rather than speed indication, and a true picture of events is not given. Figure 23 shows the variation of fluid bulk density with time at several stations in the feed line. The calculation which resulted in

this figure made use of unverified methods of estimation of mass flow and heat removal because of the presence of two-phase flow. Figure 25 shows the "g" load at the nozzle inlet manifold and figure 33 shows a sketch of the reflector outlet fluid temperature sensors. The remaining figures show pressure, fluid temperatures, material wall temperatures, or average material temperatures in the various components of the system. Figure 37 indicates that liquid hydrogen temperature exists near the run end; in reality, fog was observed during the test.

CONCLUDING REMARKS

A hasty review has been made of the data presented herein. From this review it appears that

1. The turbopump accelerated approximately as expected and showed no evidence of sticking at startup.
2. Pressure fluctuations in the reflector and nozzle passages during the initiation of flow occurred as expected. The amplitudes of these fluctuations were not, however, as severe as has been observed in other hydrogen evaporation systems.
3. A large amplitude nozzle vibration was observed during a portion of the test. This vibration is attributed to separation of flow from the surface of the nozzle.

REFERENCE

1. Lacy, D. D.; Esterly, J. R.; Straight, D. M.; Pierce, J. G.; and Humenik, F. M.: Nuclear Rocket Simulated Tests: Facility and Research Apparatus Description.

CONFIDENTIAL

TABLE I.- INSTRUMENTATION

Item No.	Description (a)	Recording Instrument				Estimated Overall Accuracy (b)	Remarks
		4 KC	10 KC	FM	Oscil.		
TR-3	T _{fl} , tank adapter	x	x			± 0.4°R at 40°R ± 0.4 ± 1.4 psi ± 1.4 psi	Calibration problem Periodic spikes in record due to Helium gas leak.
TR-5	" "		x				
TP-3	P _s , tank gas	x	x		x		
TP-5	tank adapter	x	x				
TP-6	" "	x	x				
TF-1	w, tank exit flowmeter	x	x	x			
PR-1	T _{fl} , pump inlet		x			± 0.4°R at 40°R " " " " " " " "	
PR-2	" "		x				
PR-4	T _{fl} , pump outlet	x	x		x		
PR-5	" "		x				
PR-12	T _{fl} , feed line sta. A		x				
PR-13	" " " "	x				± 6.0°R at 40°R " " " " " " " " " " " " " " " " " "	
PR-14	" " " "	x					
PR-15	" " " B	x			x		
PR-16	" " " C		x				
PR-17	" " " D	x					
PR-18	" " " D	x					
PR-19	" " " D	x					
PR-20	" " " E		x				
PR-21	" " " E	x					
PR-22	" " " E	x					
PR-25	T _{fl} , main valve	x	x	x		± 0.4°R ± 0.7 psi ± 1.4 psi " " " " " "	
PP-2	P _s , pump inlet duct	x					
PP-3	" " " "		x				
PP-12	P _s , pump outlet duct	x	x				
PP-21	P _s , feed line sta. A	x	x				
PP-22	" " " B	x	x				
PP-25	" " " C	x	x		x		
PP-26	" " " D	x	x				

CONFIDENTIAL

TABLE I.- INSTRUMENTATION, Cont'd

Item No.	Description (a)	Recording Instrument				Estimated Overall Accuracy (b)	Remarks
		4 KC	10 KC	FM	Oscil.		
NP-7	Ps, nozzle tube X=3.5	x	x			+ 1.4 psi	
NP-8	Ps, nozzle tube X=12.5	x	x			"	
NP-9	" " X=25.7	x	x			"	
NP-10	" " X=45.0	x	x	x		"	
NP-11	" " X=55.0	x	x			"	
NP-20	Ps, nozzle chamber $\theta=232$		x	x		+ .7 psi	
NP-21	" " $\theta=140$	x				"	
NP-38	Ps, nozzle throat $\theta=206$	x				"	
NP-42	Ps, nozzle exit bell X=55		x			+ .35 psi	
NT-10	T _w , nozzle tube wall X=25.7	x					
NT-15	T _{f1} , nozzle tube fluid X=11.2		x				Calibration problem.
NT-16	T _{f1} , nozzle tube wall X=44		x	x			Open circuit
NT-60	T _{f1} , nozzle chamber rake R=11.5	x	x				
NT-61	T _{f1} , nozzle chamber rake R=5.5	x		x			ISA RP 1.3 Standard Accuracy Spec.
NT-62	T _{f1} , nozzle chamber rake R=0.5	x	x				"
NT-72	T _w , inlet spider legs	x					"
NT-73	" " "	x					"
NT-74	" " "	x					"
NT-75	" " "	x					"
NT-76	" " "	x					"
NT-77	" " "	x					"
NA-0	"g", nozzle manif. $\theta=0^\circ$				x		
RR-607	T _{f1} , reflector inlet, $\theta=45$		x	x		+ 6.0°R	
RR-610	" " $\theta=115$		x			+ 0.4°R	
RR-612	" " $\theta=235$		x			+ 6.0°R	
RR-619	" " exit $\theta=45$		x			"	
RR-622	" " $\theta=115$		x	x		"	
RR-624	" " $\theta=285$		x			"	

CONFIDENTIAL

TABLE I.- INSTRUMENTATION, Cont'd

Item No.	Description (a)	Recording Instrument				Estimated Overall Accuracy (b)	Remarks
		4 KC	10 KC	FM	Oscil.		
RP-28	Ps, fuel ele. inlet plen. R=17	x				+ 1.35 psi	
RP-31	" " " " R=0	x				"	
RP-32	" " " " R=10	x				"	
RP-121	Ps, flow separator R=16	x				"	
RP-140	Ps, refl. inlet $\phi=38$	x		x		"	
RP-141	" " $\phi=158$	x				"	
RP-146	Ps, refl. exit $\phi=158$	x				"	
RT-1	T _m , fuel element No. 1	x				ISA RP 1.3 Standard Accuracy Spec.	
RT-2	" " " "	x				"	
RT-3	" " " "	x				"	
RT-4	" " " "	x				"	
RT-5	" " " "	x				"	
RT-8	" " " " 7	x				"	
RT-13	" " " " 11	x				"	
RT-18	" " " " 14	x				"	
RT-23	" " " " 16	x				"	
RT-28	" " " " 18	x				"	
RT-31	T _m , module R=0.62	x				"	
RT-32	" " " "	x				"	
RT-33	" " " "	x				"	
RT-34	" " " "	x				"	
RT-35	" " " "	x				"	
RT-43	" " R=9.62	x				"	
RT-48	" " R=16.2	x				"	
RT-74	T _m , graphite cylinder $\phi=170^\circ$	x				"	
RT-75	" " " "	x				"	
RT-76	" " " "	x				"	
RT-77	" " " "	x				"	
RT-78	" " " "	x				"	
RT-79	" " " "	x				"	

TABLE I. INSTRUMENTATION, Cont'd

Item No.	Description (a)	Recording Instrument				Estimated Overall Accuracy (b)	Remarks	
		4 KC	10 KC	FM	Oscil.			
RT-170	T _m , refl. segment at $\theta=180$	x	x			ISA RP 1.3 Standard Accuracy Spec.	Coded out in data reduction.	
RT-172	" " " "	x	x					
RT-175	" " " "	x	x					
RT-176	" " " "	x	x					
RT-178	" " " "	x	x					
RT-181	" " " "	x	x					
RT-182	" " " "	x	x					
RT-184	" " " "	x	x					
RT-187	" " " "	x	x					
RT-188	" " " "	x	x					
RT-193	" " " "	x	x					
RT-208	" " " " $\theta=240$	x	x					
RT-290	T _m , control rod at $\theta=180$	x	x					Equivalent measurement at $\theta=180$ was open circuit.
RT-291	" " " "	x	x					
RT-292	" " " "	x	x					
RT-293	" " " "	x	x					
RT-294	" " " "	x	x					
RT-295	" " " "	x	x					
RT-296	" " " "	x	x					
RT-297	" " " "	x	x					
RT-298	" " " "	x	x					
RT-342	T _{f1} , core sup. plate R=0	x						
RT-361	T _m , pressure shell $\theta=170$	x						
RT-362	" " " "	x						
RT-363	" " " "	x						
RT-379	" " " "	x						
RT-380	" " " "	x						
RT-381	" " " "	x						
RT-392	T _{f1} , core sup. plate R=17.1	x						

TABLE I.- INSTRUMENTATION, Cont'd

Item No.	Description (a)	Recording Instrument			Estimated Overall Accuracy (b)	Remarks
		4 KC	10 KC	FM Oscil.		
RM-317	Tf1, control rod Z=1.25	x	x	x	+ 5.0°R	Calibration error of about 12°R.
RM-318	" " Z=13.25				"	Open circuit in sensor.
RM-319	" " Z=28.25	x	x	x	"	Calibration error of about 12°R
RM-320	" " Z=37.25	x	x	x	"	"
RM-321	" " Z=45.25	x	x	x	"	"
RM-322	" " Z=51.25	x	x	x	"	"
EP-1	Ps, ejector inlet	x			+ 0.2 psi	"

(a) Tf1 = fluid temperature

Ps = static pressure

W = flow rate

ΔP = outside wall temperature

T_w" = outside wall temperature

"g" = 32.2 ft/sec² acceleration

T_m = temperature within material

(embedded thermocouple)

(b) Accuracy estimate includes errors due to calibration, repeatability, data acquisition systems, and data reduction.

LIST OF FIGURES

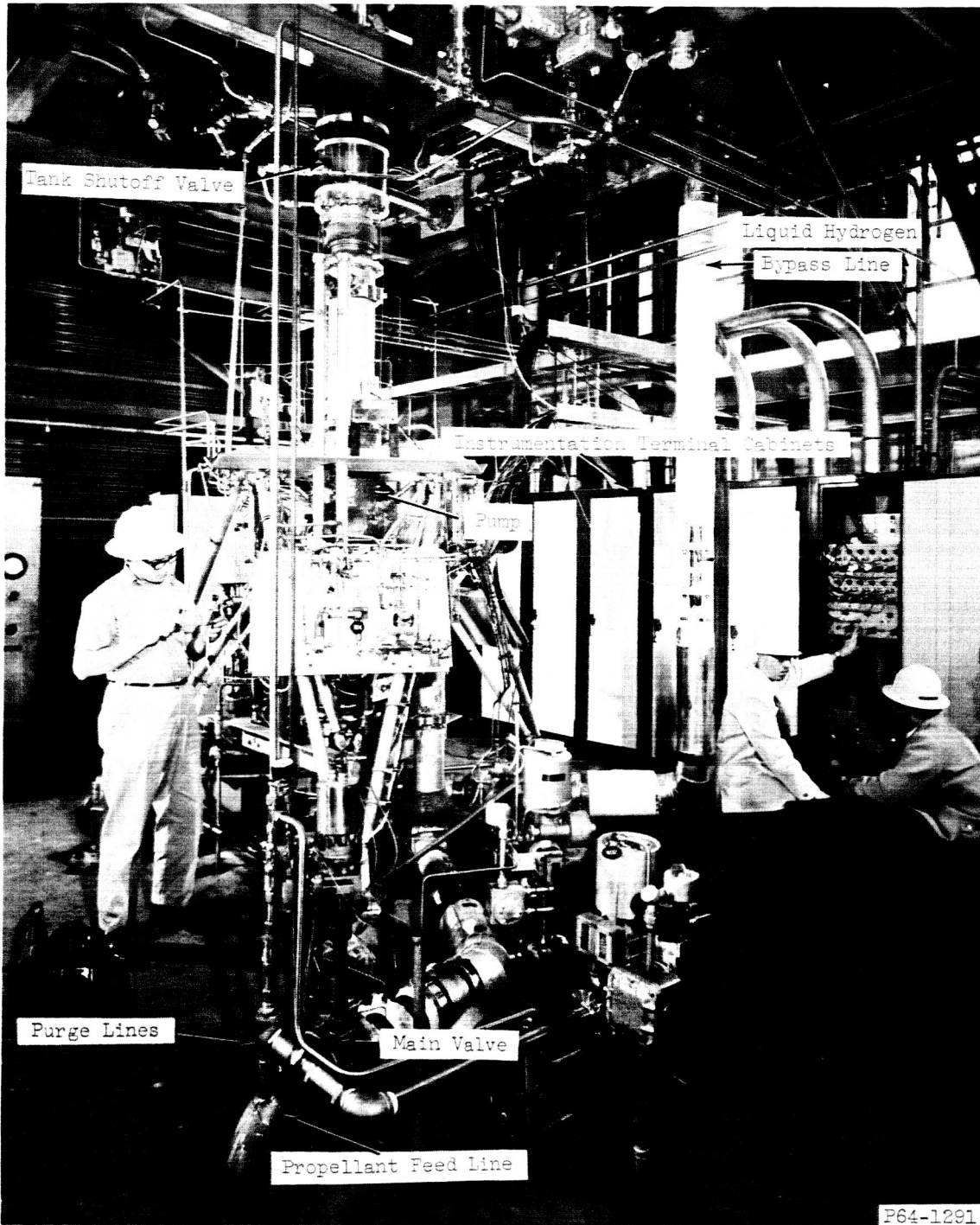
- 1(a) - Mark IX liquid hydrogen turbopump installation.
- 1(b) - Hydrogen feed line, nozzle, and reactor.
- 2 - Nuclear rocket cold flow experiment in B-1 facility.
- 3 - Nuclear rocket cold flow tests nozzle showing major instrumentation stations, B-1 facility.
- 4(a) - Top view of nuclear rocket cold flow tests reactor showing major instrumentation stations, B-1 facility.
- 4(b) - Side view of nuclear rocket cold flow tests reactor showing major instrumentation stations, B-1 facility.
- 5 - Variation of flow rate with time at two stations in the system.
- 6 - Pump inlet static pressure versus time.
- 7 - Pump discharge static pressure versus time.
- 8 - Nozzle inlet manifold static pressure versus time.
- 9 - Reflector inlet manifold static pressure versus time.
- 10 - Reflector exit manifold static pressure versus time.
- 11 - Core inlet static pressure versus time.
- 12 - Nozzle chamber static pressure versus time.
- 13 - Pump inlet fluid temperature versus time.
- 14 - Pump discharge fluid temperature versus time.
- 15 - Nozzle inlet manifold fluid temperature versus time.
- 16 - Reflector inlet manifold fluid temperature versus time.
- 17 - Reflector exit manifold fluid temperature versus time.
- 18 - Core inlet manifold fluid temperature versus time.
- 19 - Nozzle chamber fluid temperature versus time.

LIST OF FIGURES, Cont'd

- 20 - Variation of static pressure throughout the system at various times.
- 21 - Variation of fluid temperature throughout the system at various times.
- 22 - System startup history of Mark IX turbopump.
- 23 - Variation of bulk fluid density with time at several stations in the feed system piping.
- 24 - Inlet pipe wall temperature at station C versus time.
- 25 - Vibration "g" load at nozzle inlet manifold.
- 26 - Nozzle wall temperature versus time on exhaust side.
- 27 - Static pressure difference between nozzle tube outlet and reflector inlet plenum.
- 28 - Reactor pressure vessel average temperature versus time.
- 29 - Main aluminum reflector piece average temperature versus time.
- 30 - Average aluminum control rod temperature versus time.
- 31 - Average inner graphite reflector cylinder temperature versus time.
- 32 - Variation of fluid temperature with time at five lengthwise stations in the control rod clearance annulus.
- 33 - Reflector outlet sketch showing location of fluid temperature sensors.
- 34 - Static pressure difference between reflector outlet plenum and core support plate inlet plenum.
- 35 - Average graphite core module temperature versus time for a module at the center of the reactor.
- 36 - Average graphite fuel element temperature versus time for a fuel element at the center of the reactor.
- 37 - Radial fluid temperature profile at core outlet
- 38 - Radial temperature profile of graphite core material at several times during cooldown.

SECRET

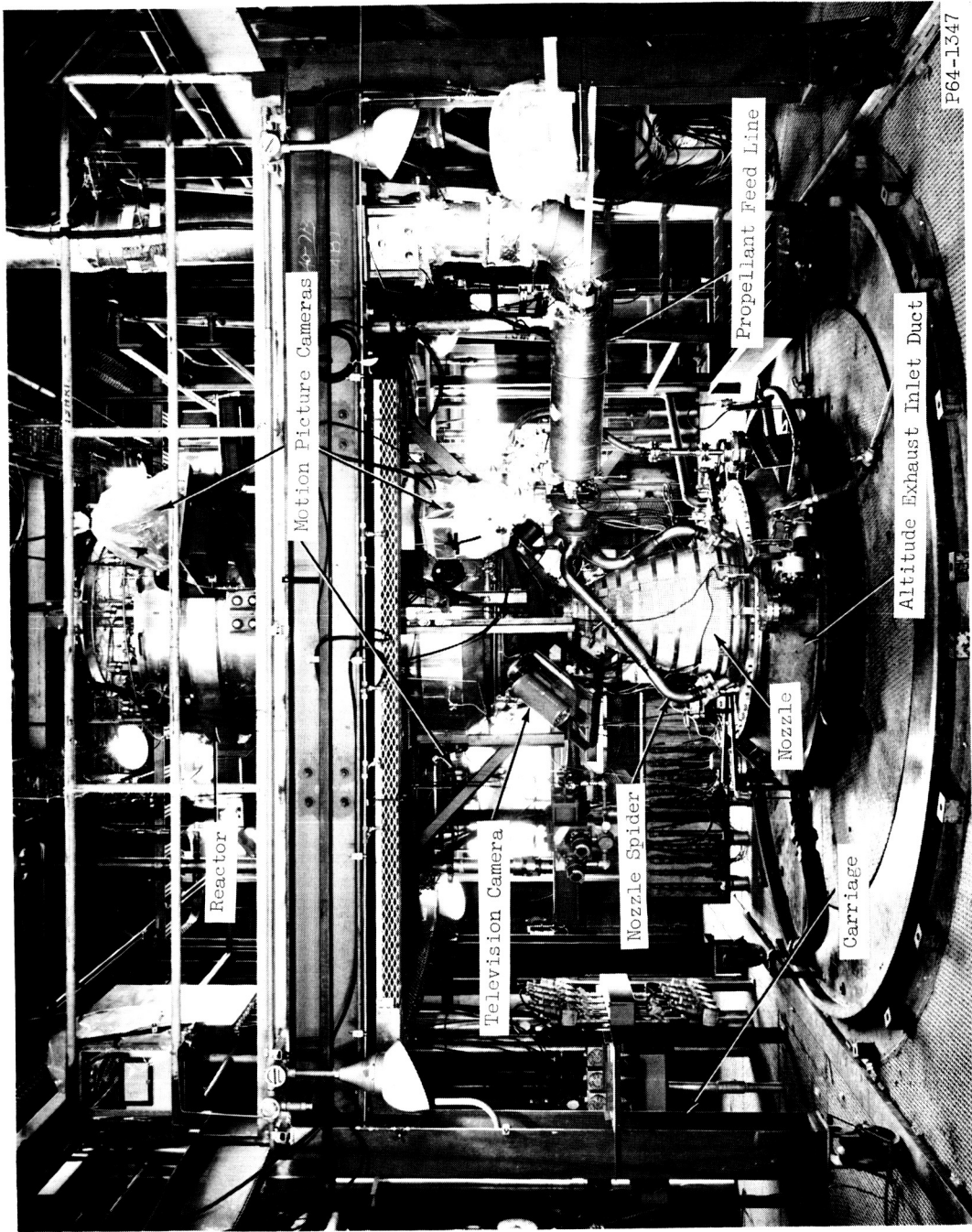
E-2673



(a) Mark IX liquid hydrogen turbopump installation.

Figure 1. - B-1 cold flow experiment.

SECRET



P64-1347

(b) Hydrogen feed line, nozzle, and reactor.

Figure 1. - Concluded. B-1 cold flow experiment.

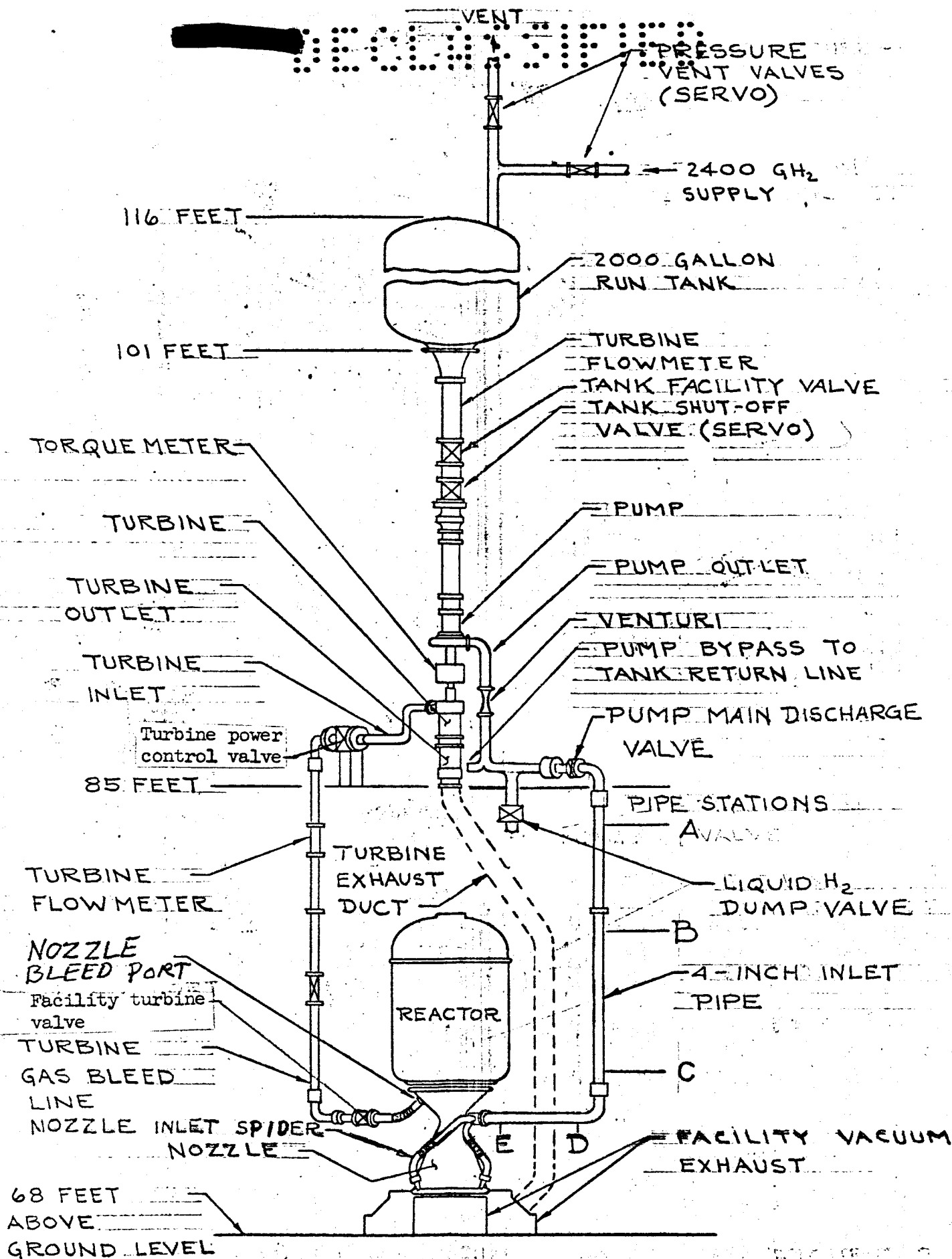


FIGURE 2 Nuclear Rocket Cold Flow Experiment in B-1

CONFIDENTIAL

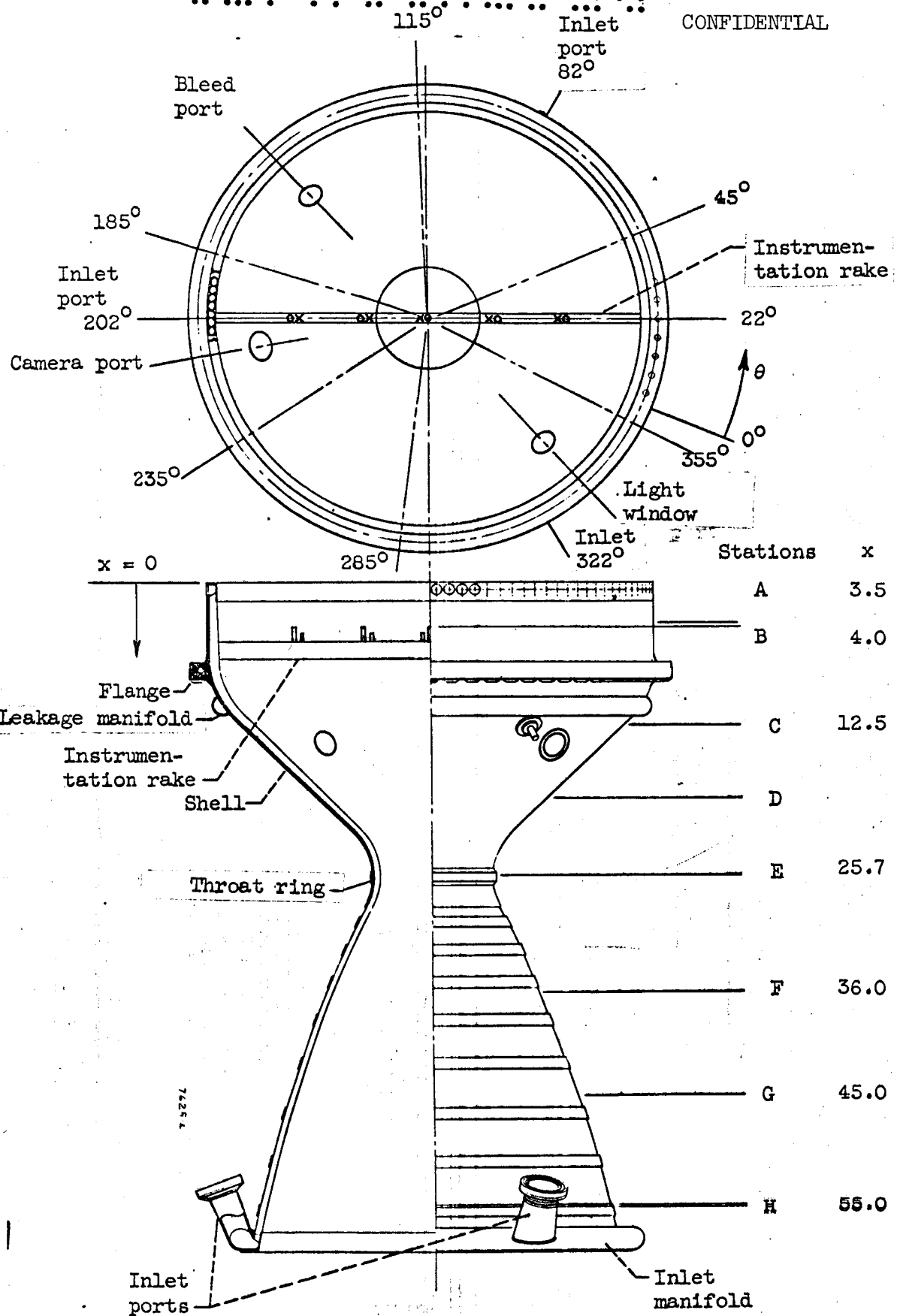
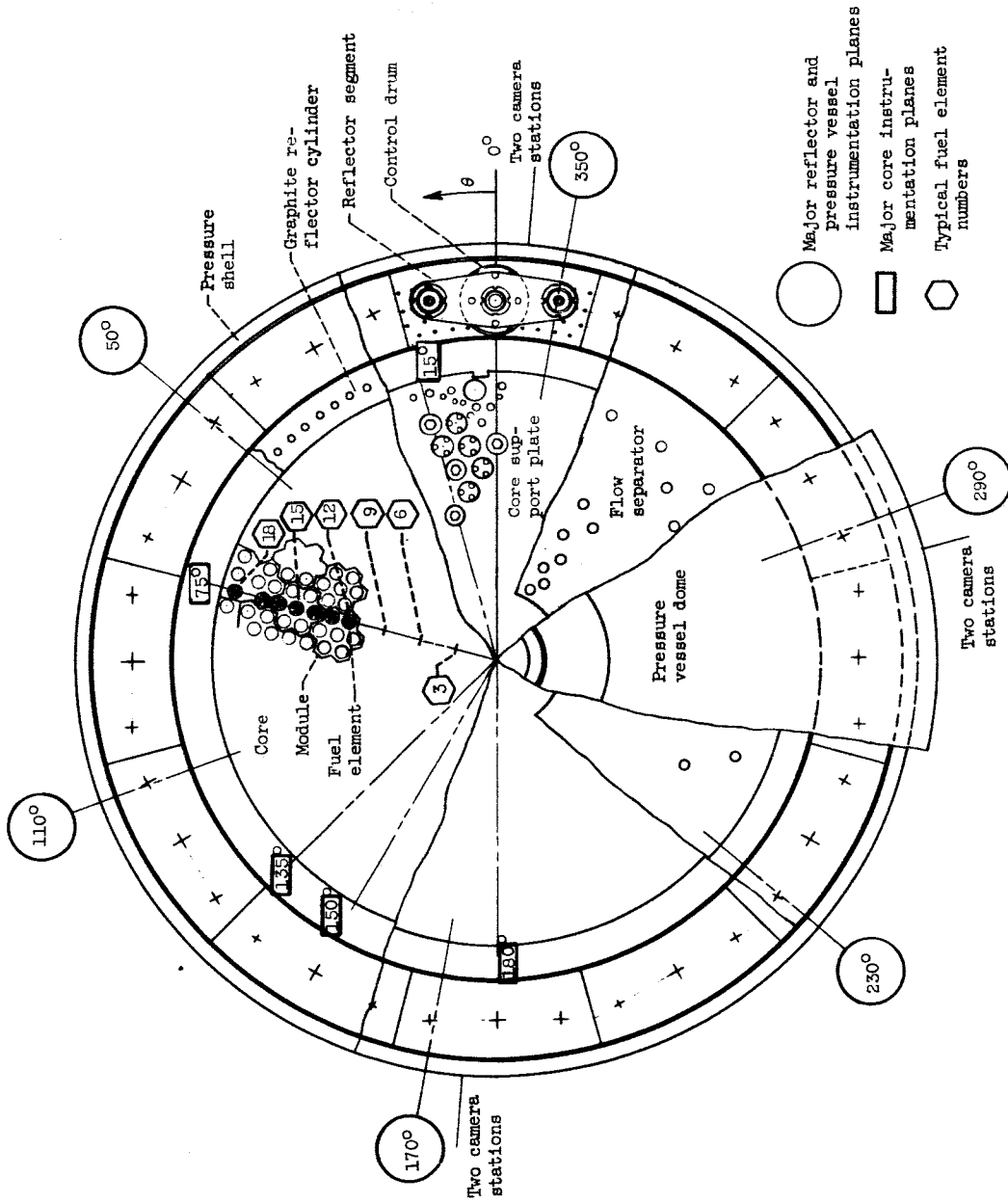


Figure 3. - Nuclear rocket cold-flow tests nozzle showing major instrumentation stations, B-1 facility.



(a) Top view.

Figure 4. - Nuclear rocket cold-flow tests reactor showing major instrumentation stations, B-1 facility.

CONFIDENTIAL

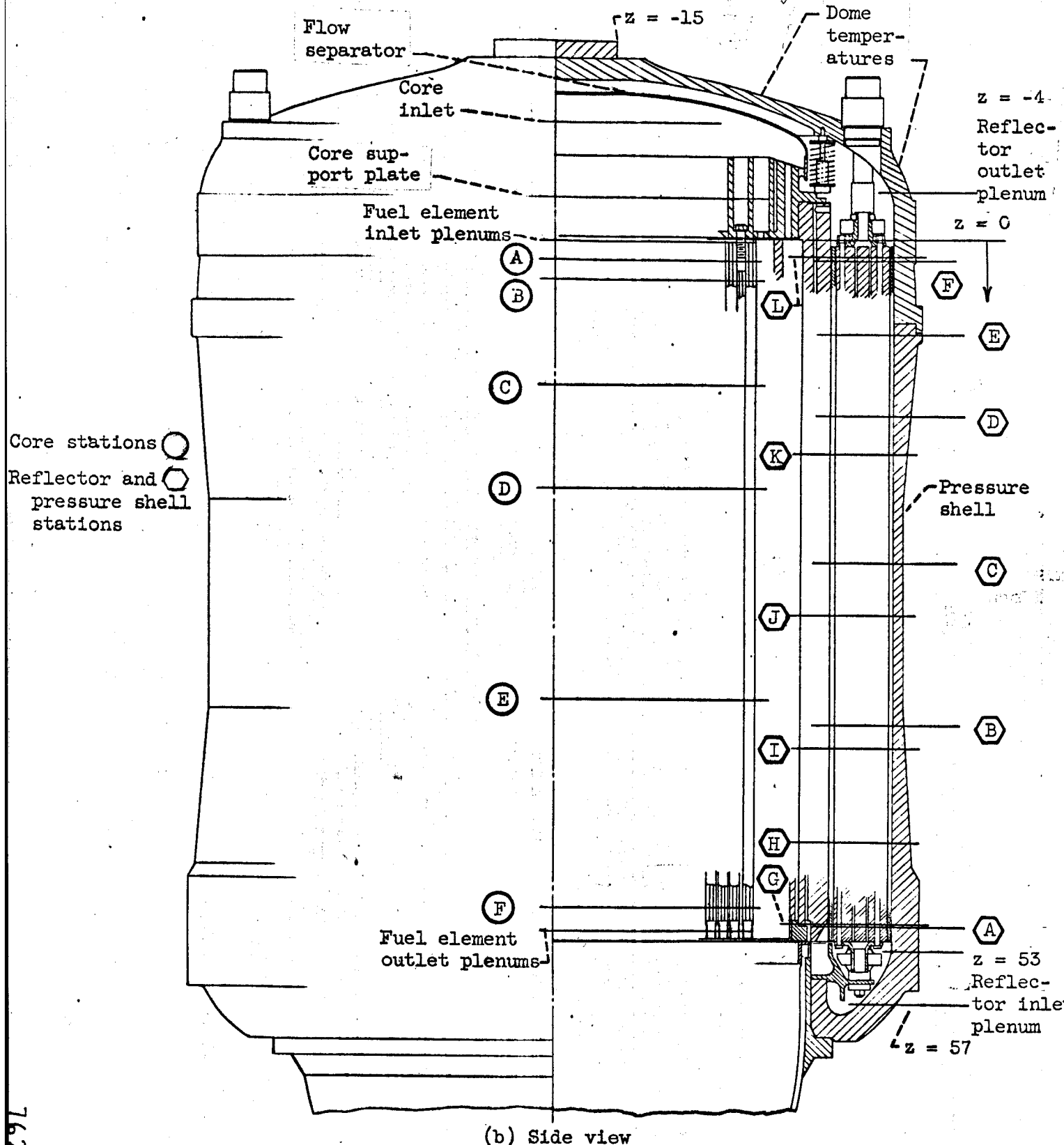


Figure 4. - Concluded. Nuclear rocket cold-flow tests reactor showing major instrumentation stations, B-1 facility.

7629-1

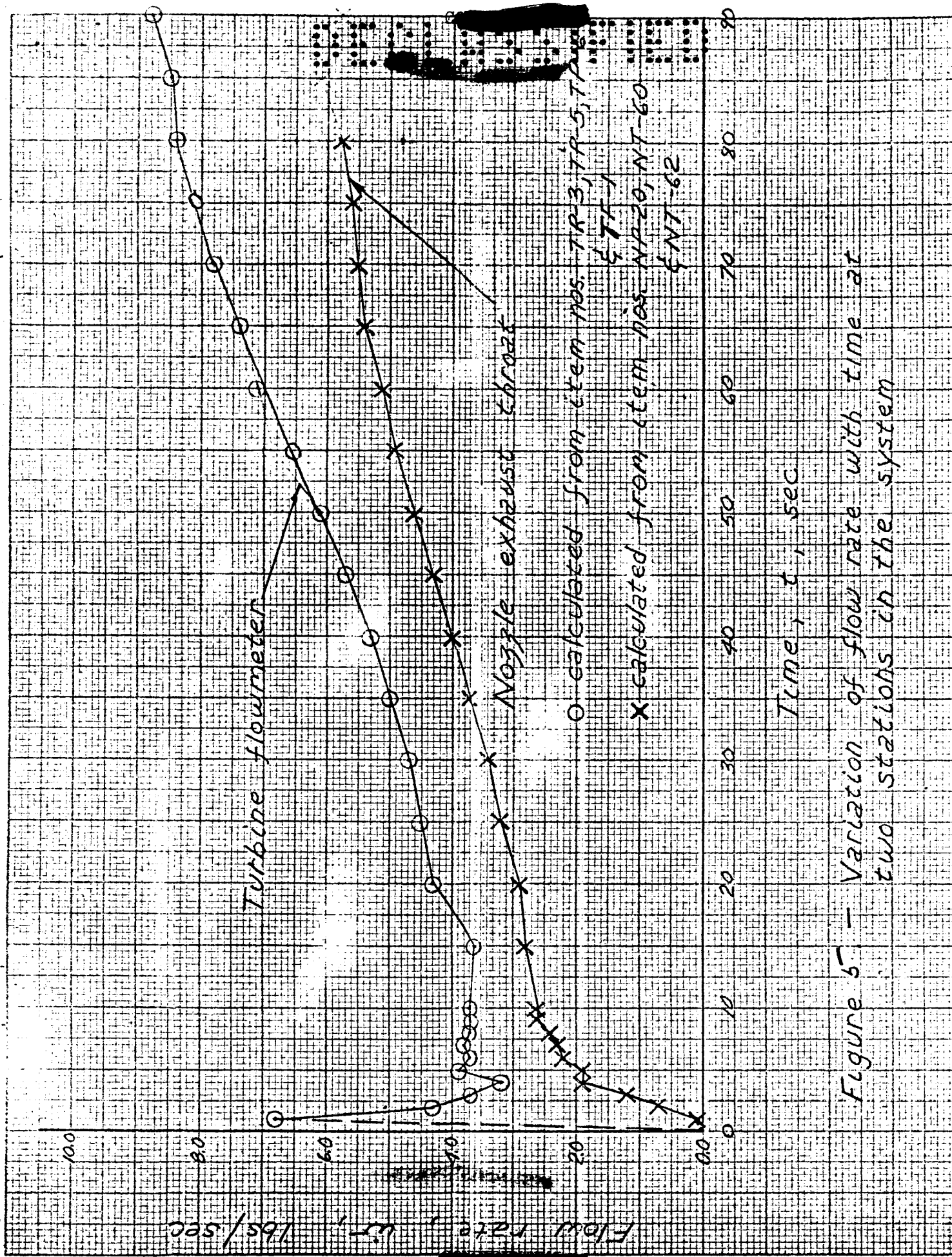


Figure 5 - Variation of flow rate with time at two stations in the system

03 70 00 00

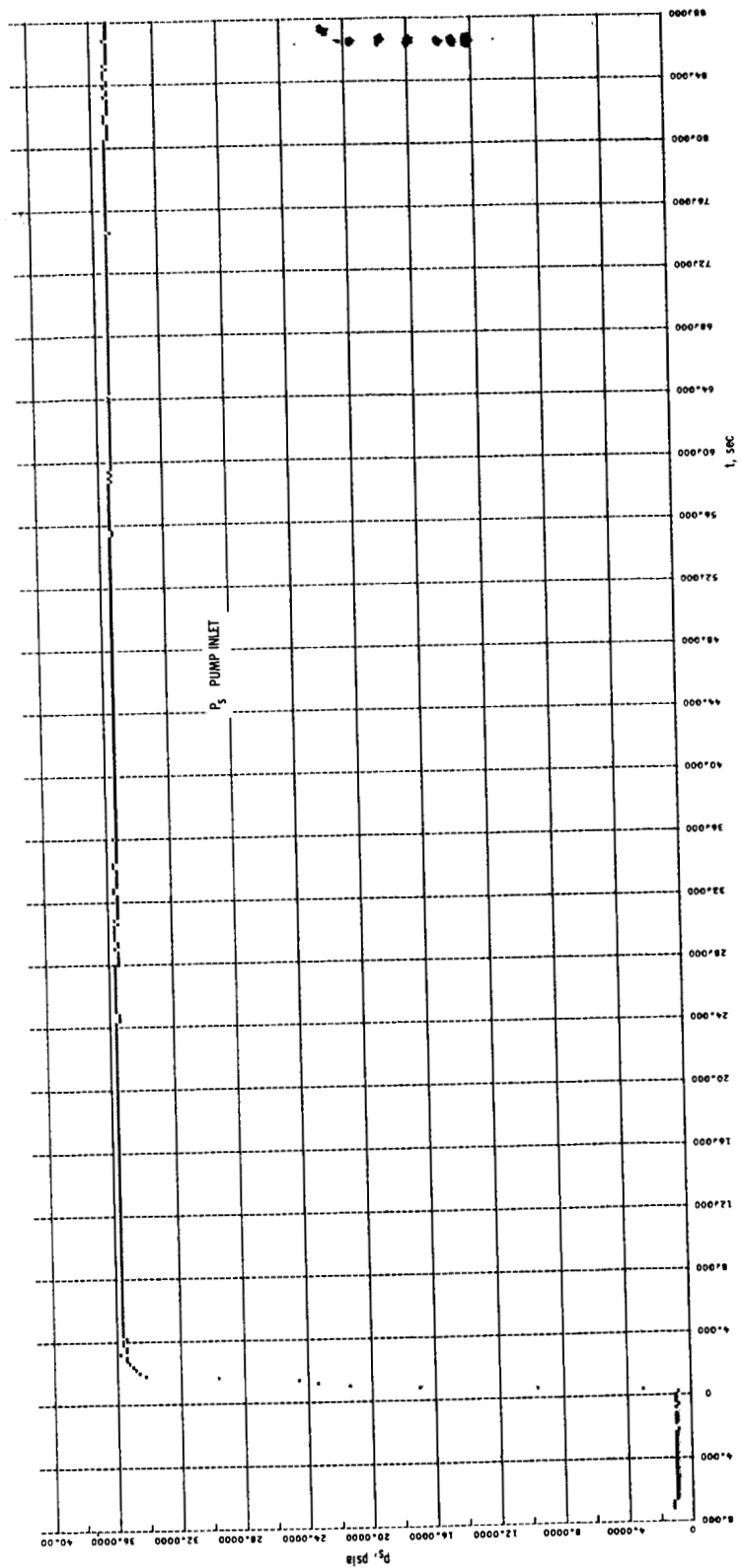


Figure 6. - Pump Inlet static pressure versus time (Item no. PP 3).

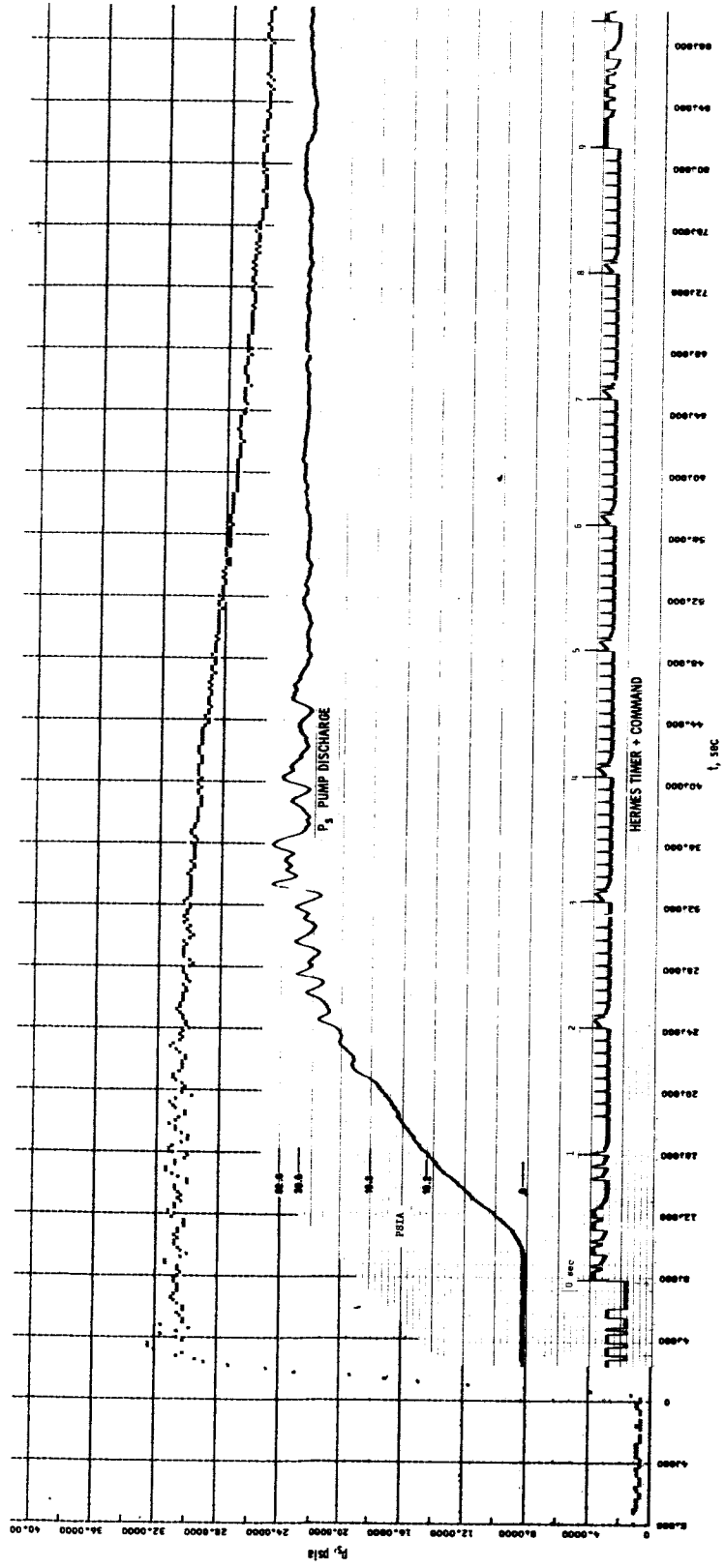


Figure 7. - Pump discharge static pressure versus time (Item no. pp. 34).

SECRET

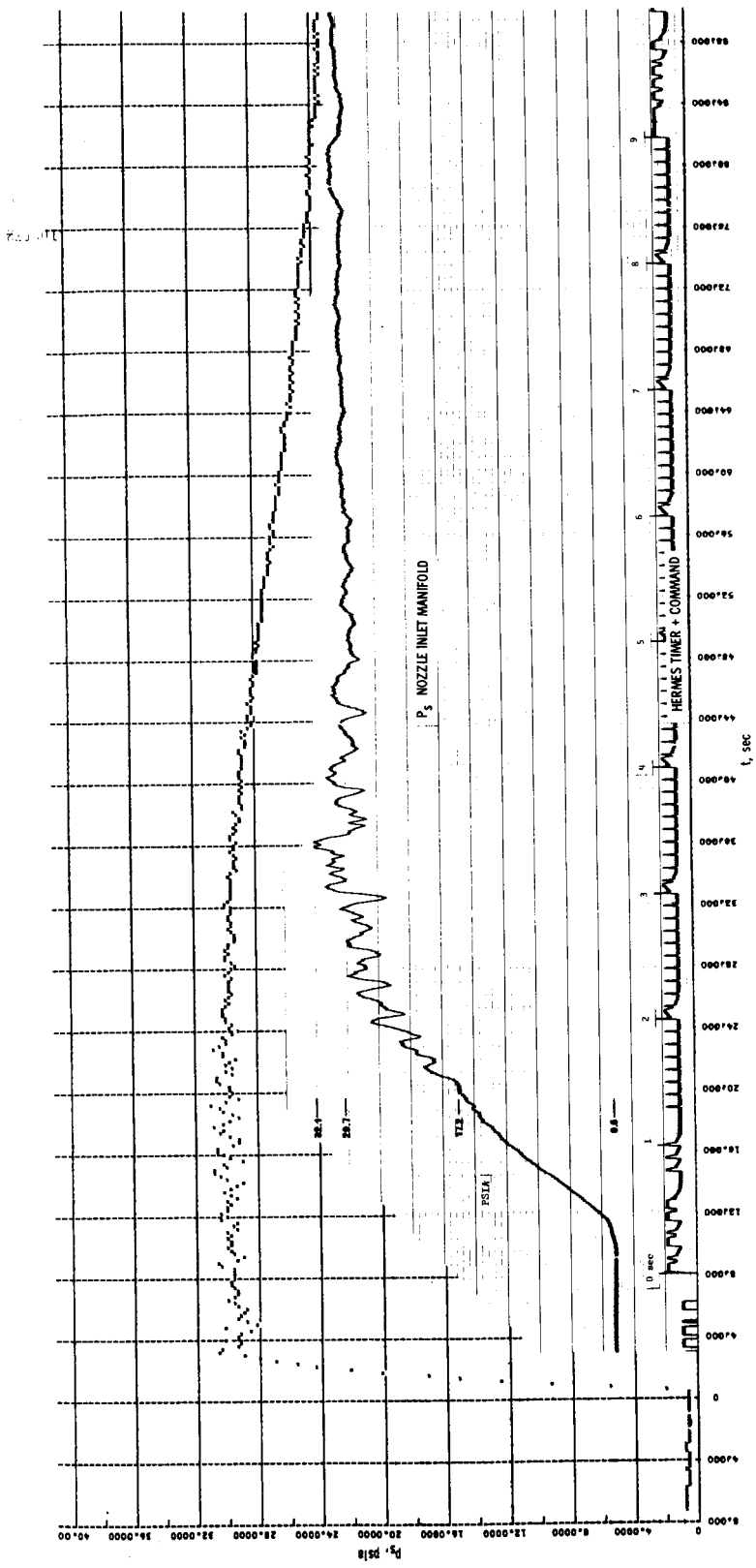


Figure 8. - Nozzle inlet manifold static pressure versus time (Item no's. NP 3 and NP 52).

SECRET

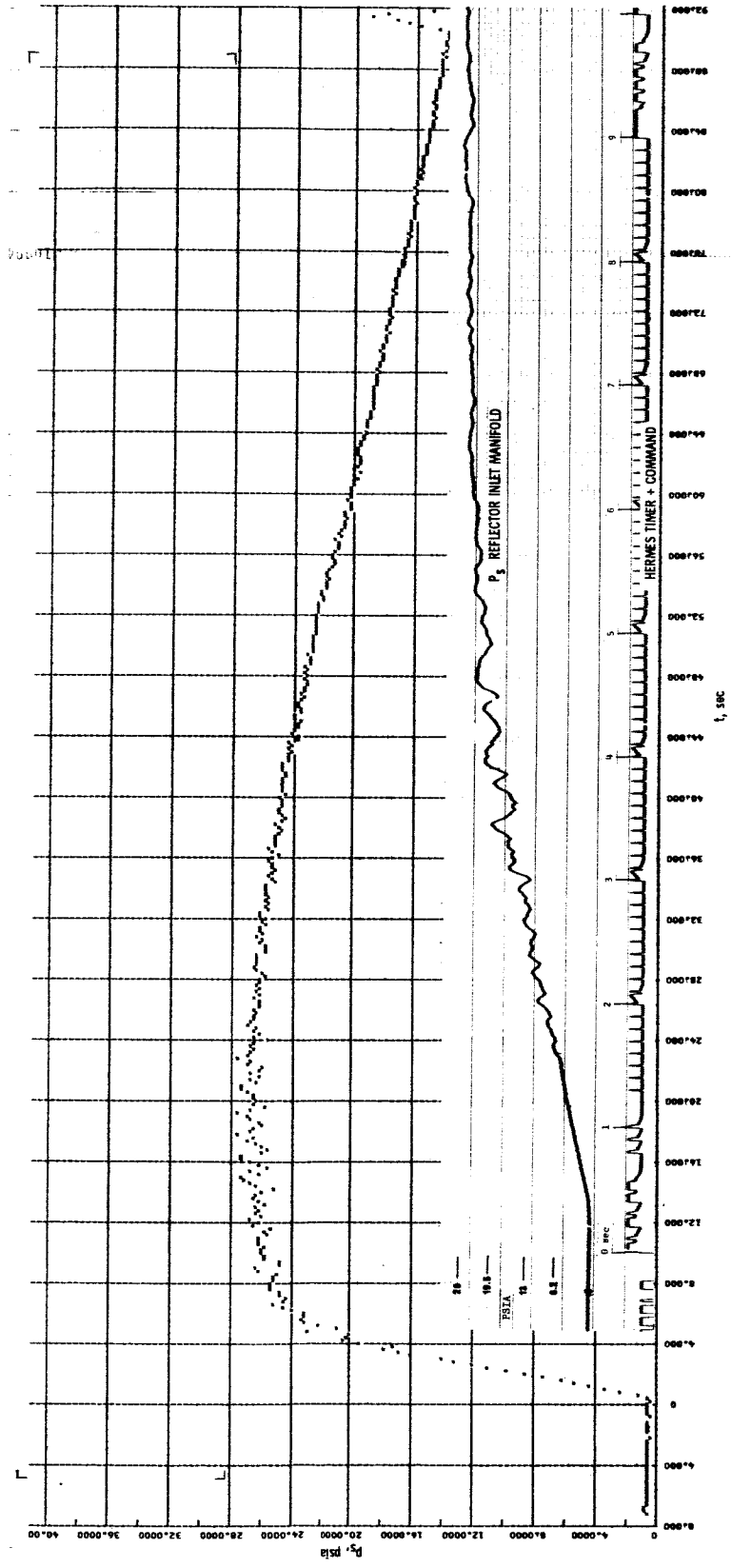


Figure 9. - Reflector Inlet manifold static pressure versus time (Item no's. RP 140 and RP 141).

SECRET

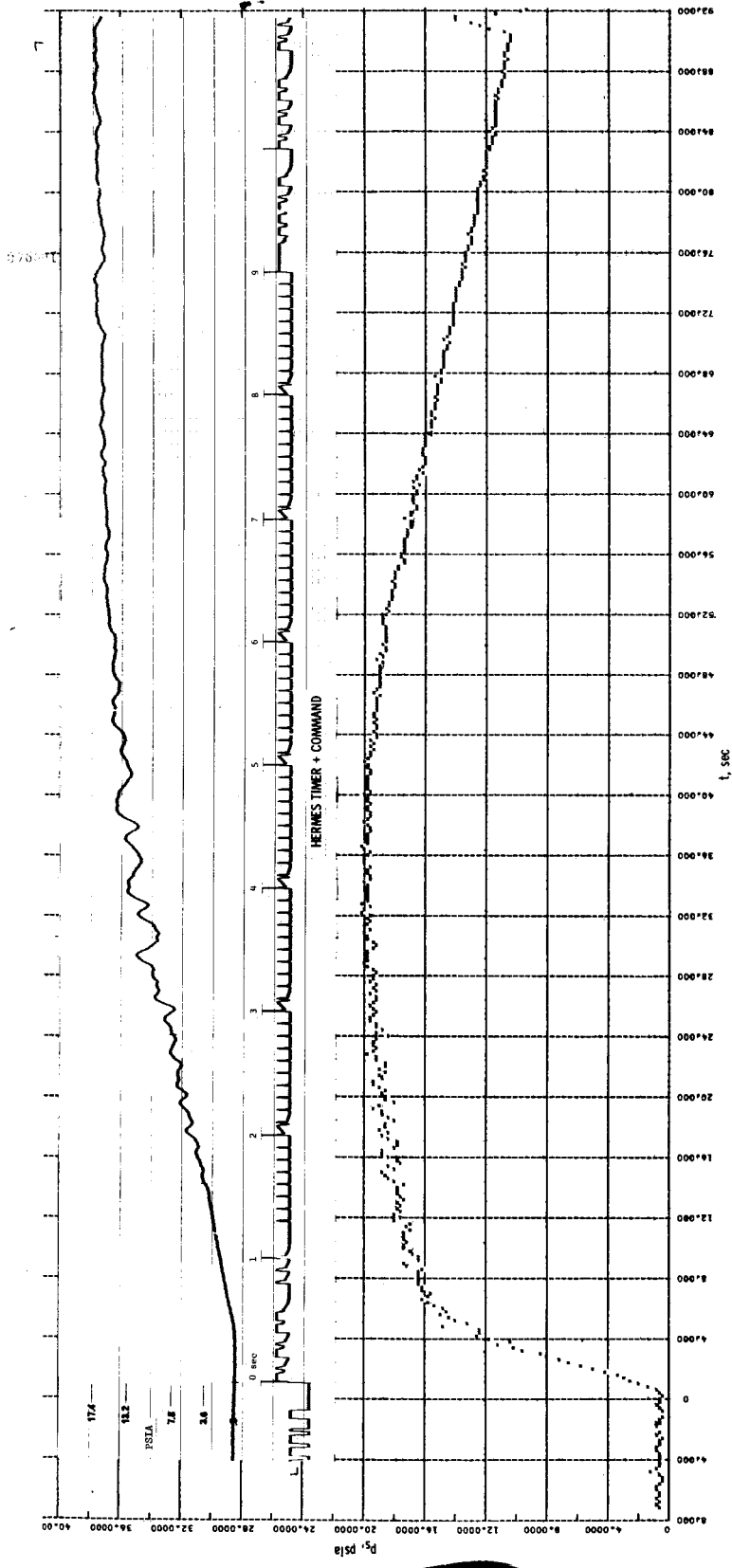


Figure 10. - Reflector exit manifold static pressure versus time (item no's, RP 145 and RP 146).

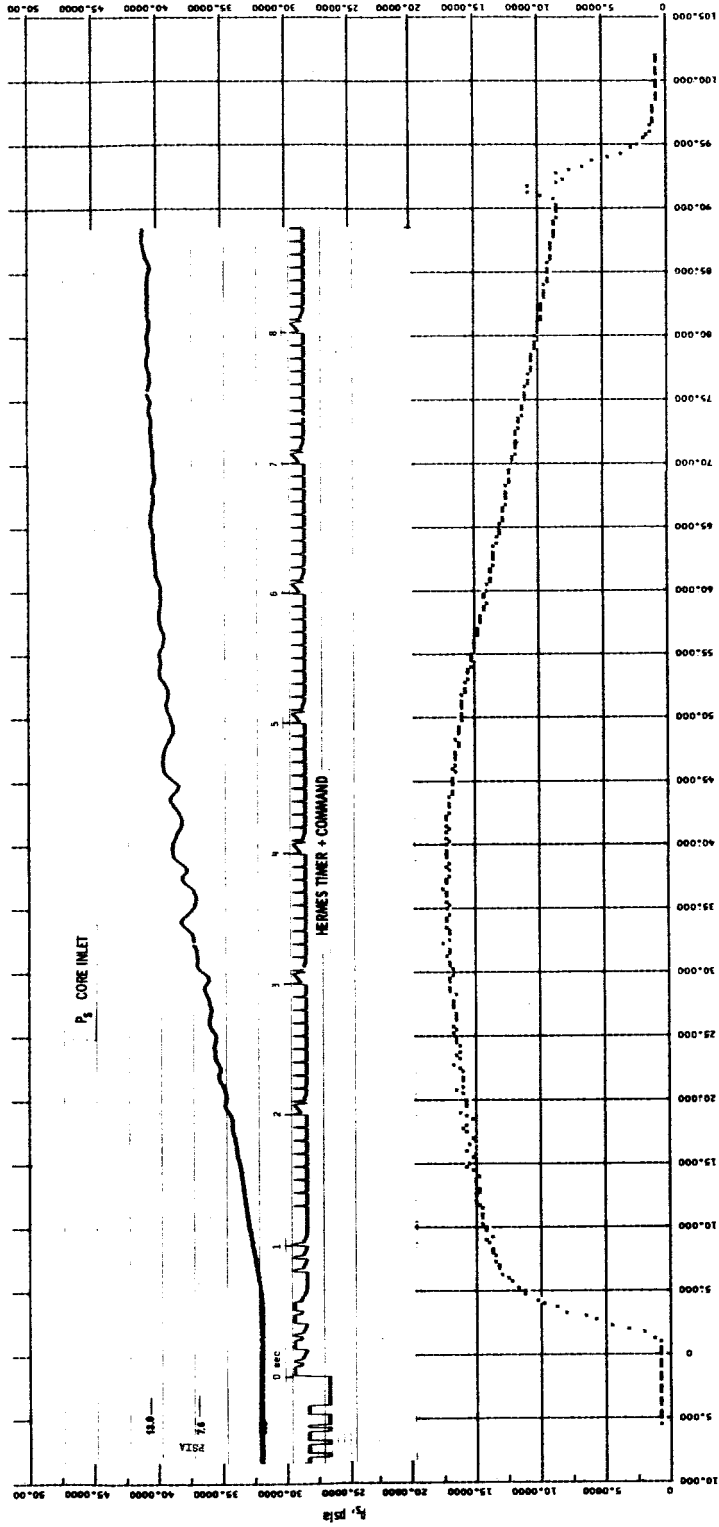


Figure 11. - Core inlet static pressure versus time (Item nos. RP 28, RP 31, RP 32, and RP 123).

SECRET

SECRET

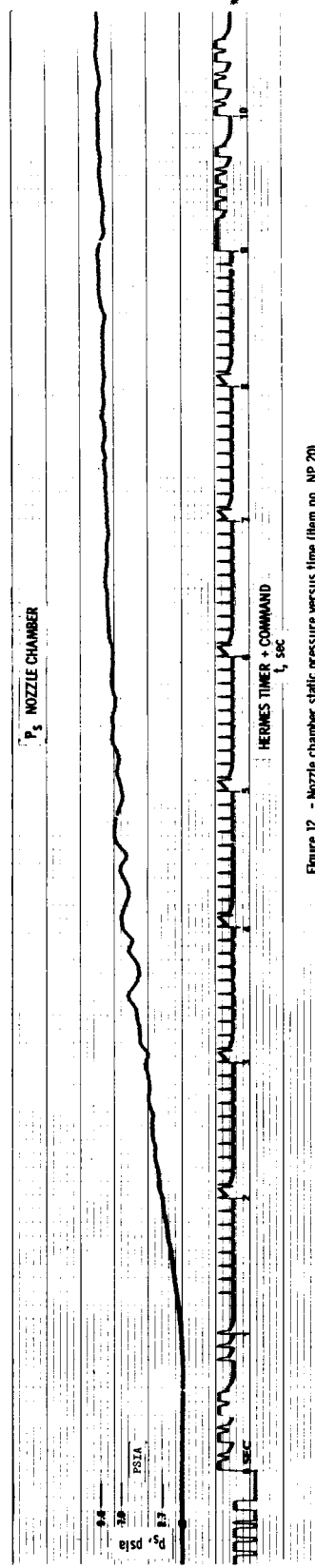


Figure 12. - Nozzle chamber static pressure versus time (item no. NP 20).

SECRET

E-2673

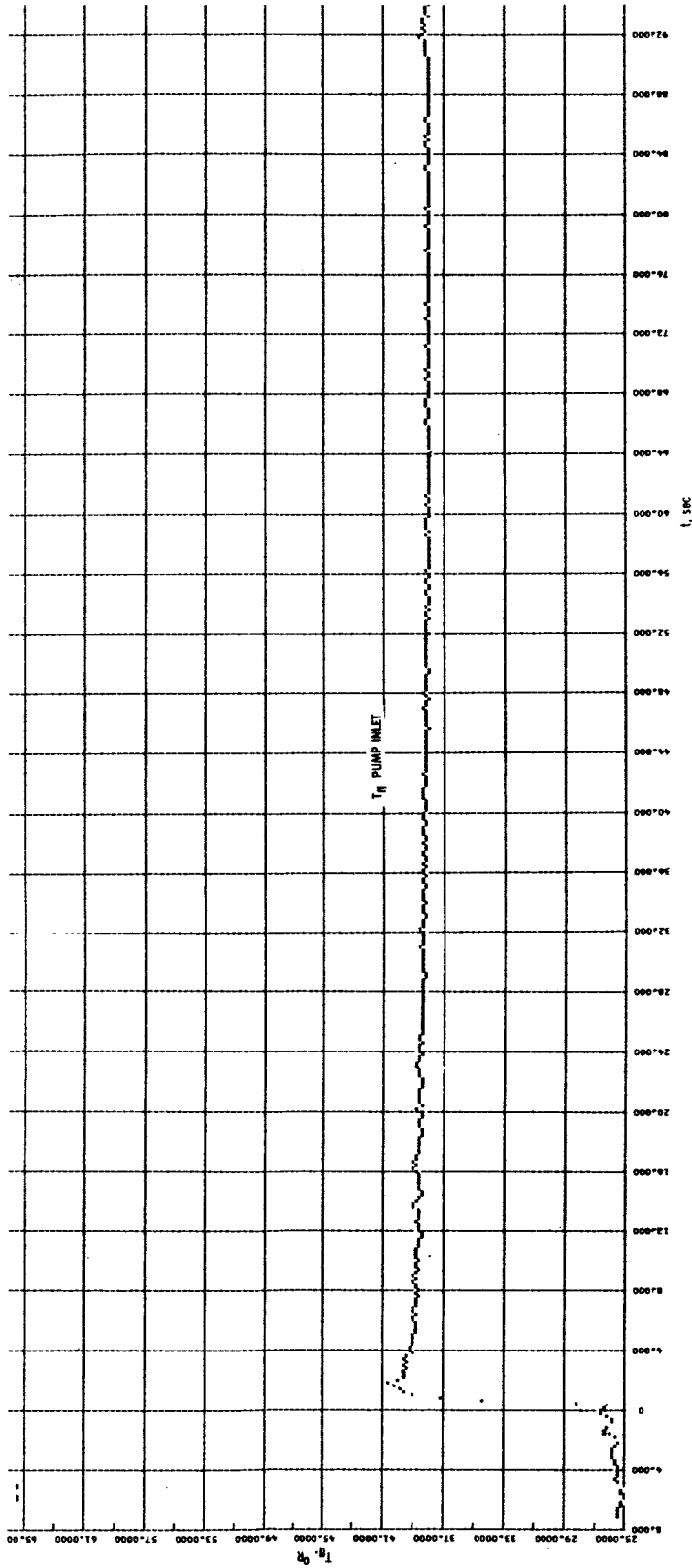


Figure 13. - Pump Inlet fluid temperature versus time (Item no. PK 1).

SECRET

0171000000

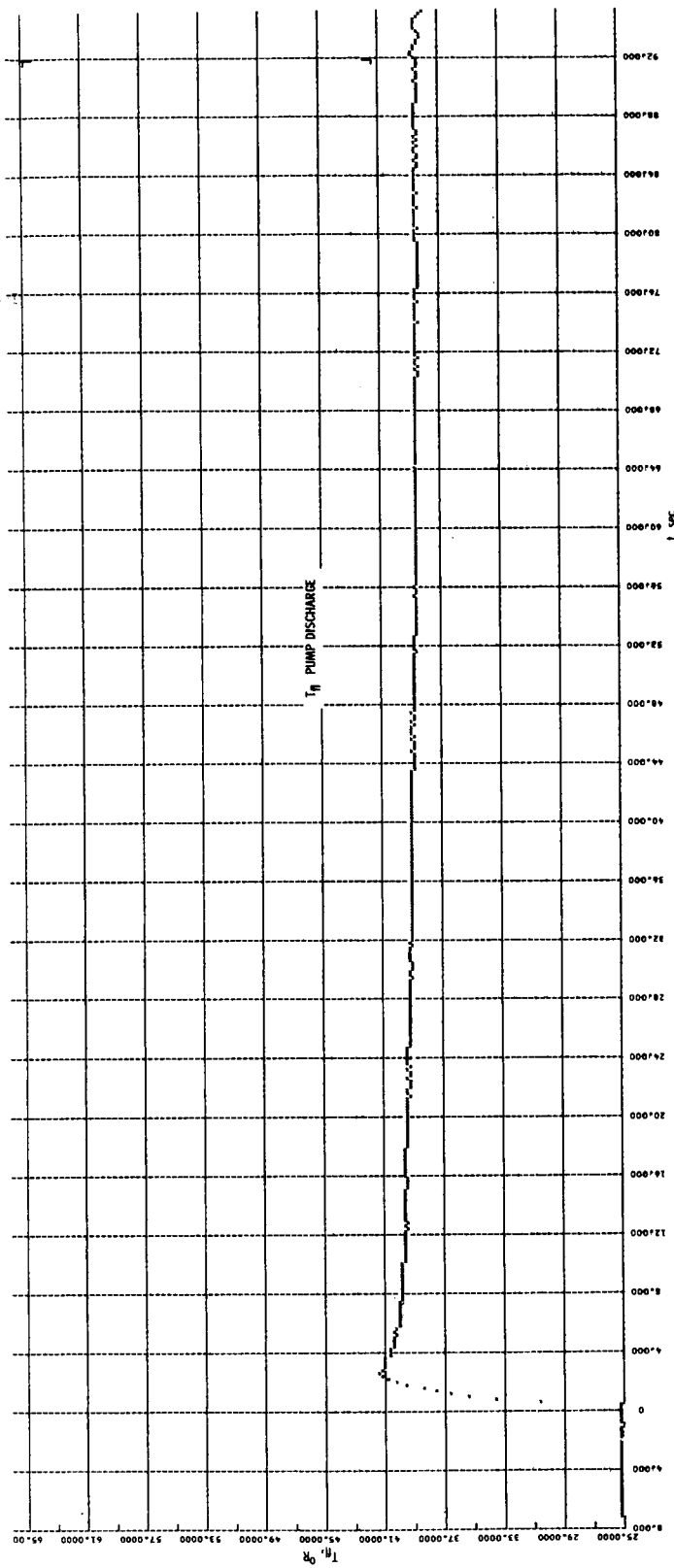


Figure 1A - Pump discharge fluid temperature versus time (Item no. PR 4).

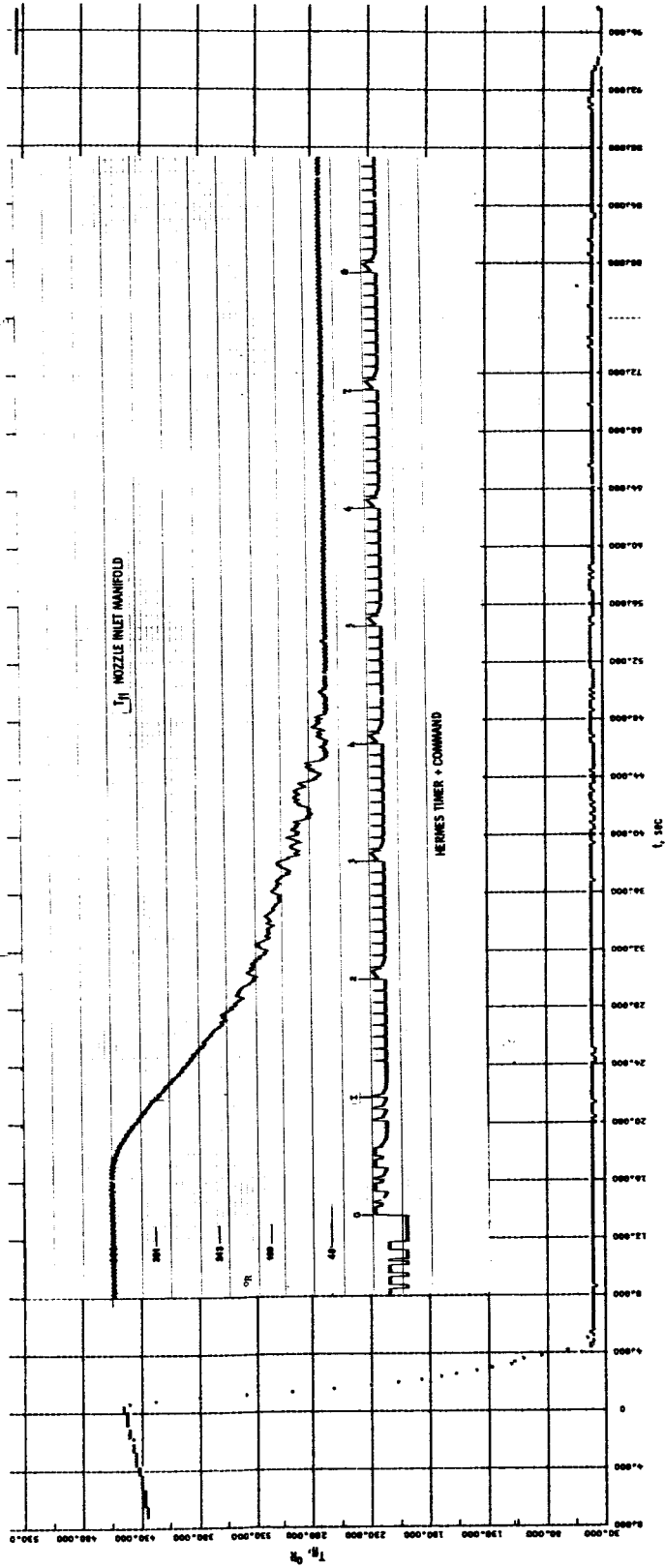


Figure 15. - Nozzle inlet manifold fluid temperature versus time (film no. NR 11).

SECRET

REFLECTOR

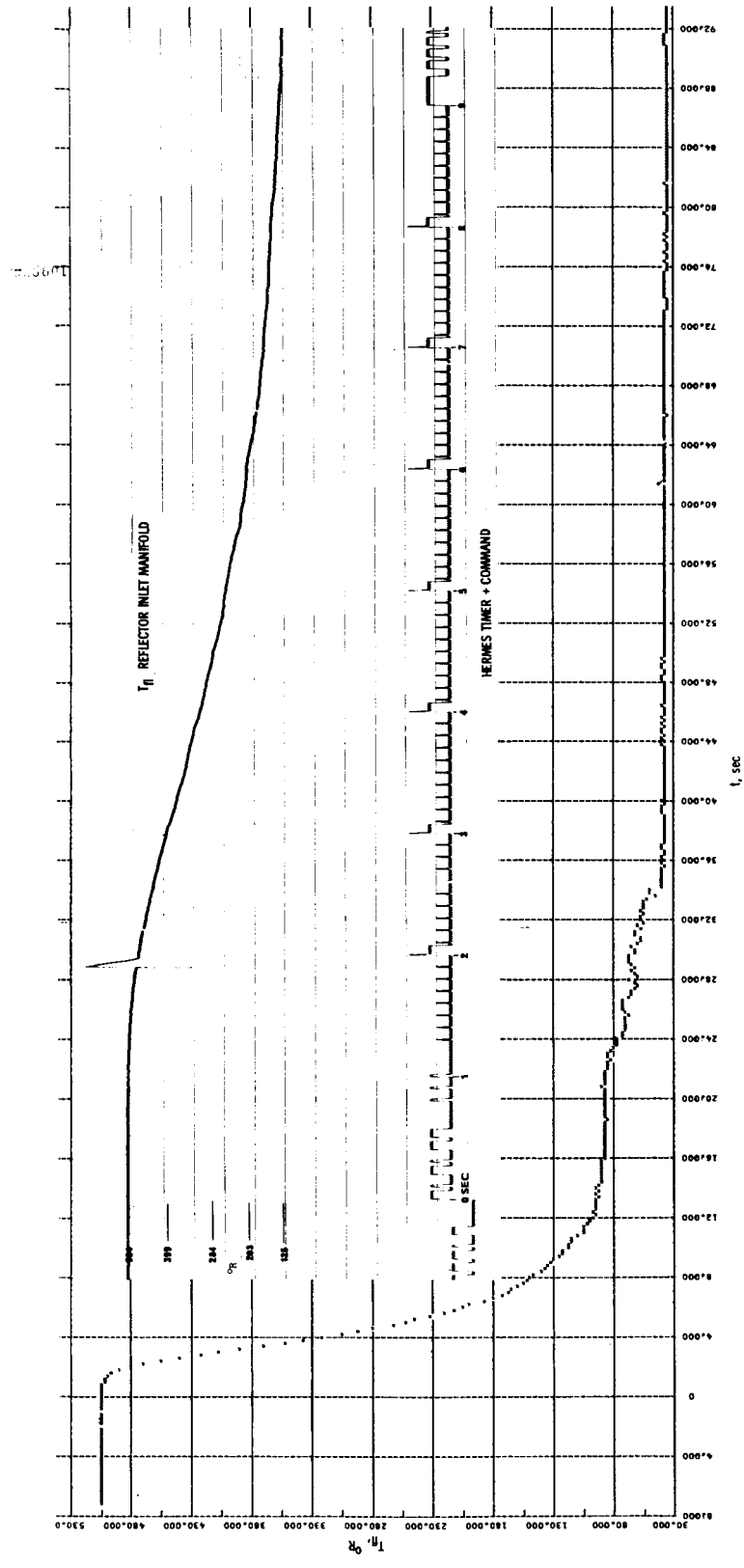


Figure 16. - Reflector inlet manifold fluid temperature versus time (item no. RR 607).

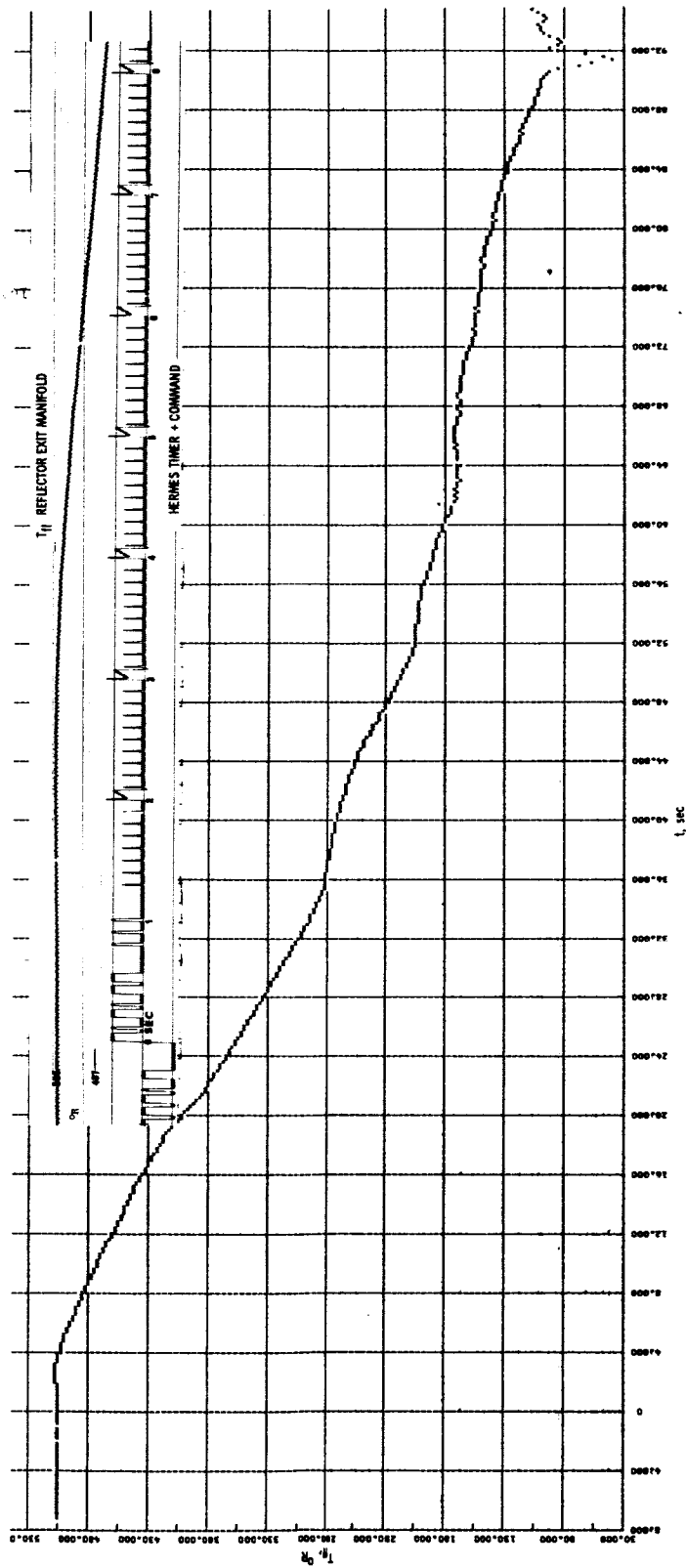


Figure 17. - Reflector exit manifold fluid temperature versus time (Item no's. RR 619 and RR 622).

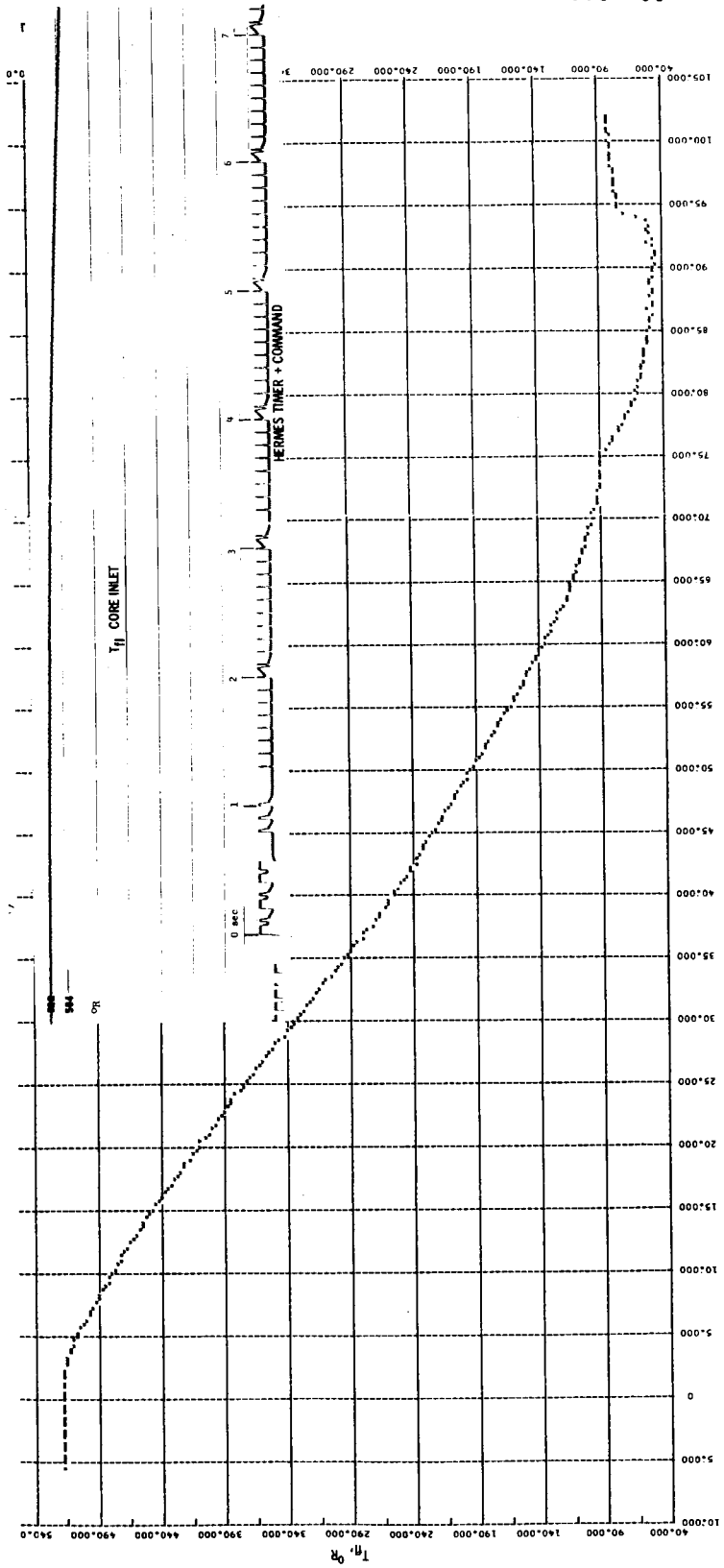


Figure 1B. - Core Inlet Fluid Temperature versus time (Item no's. RT 342, RT 344, and RT 392).

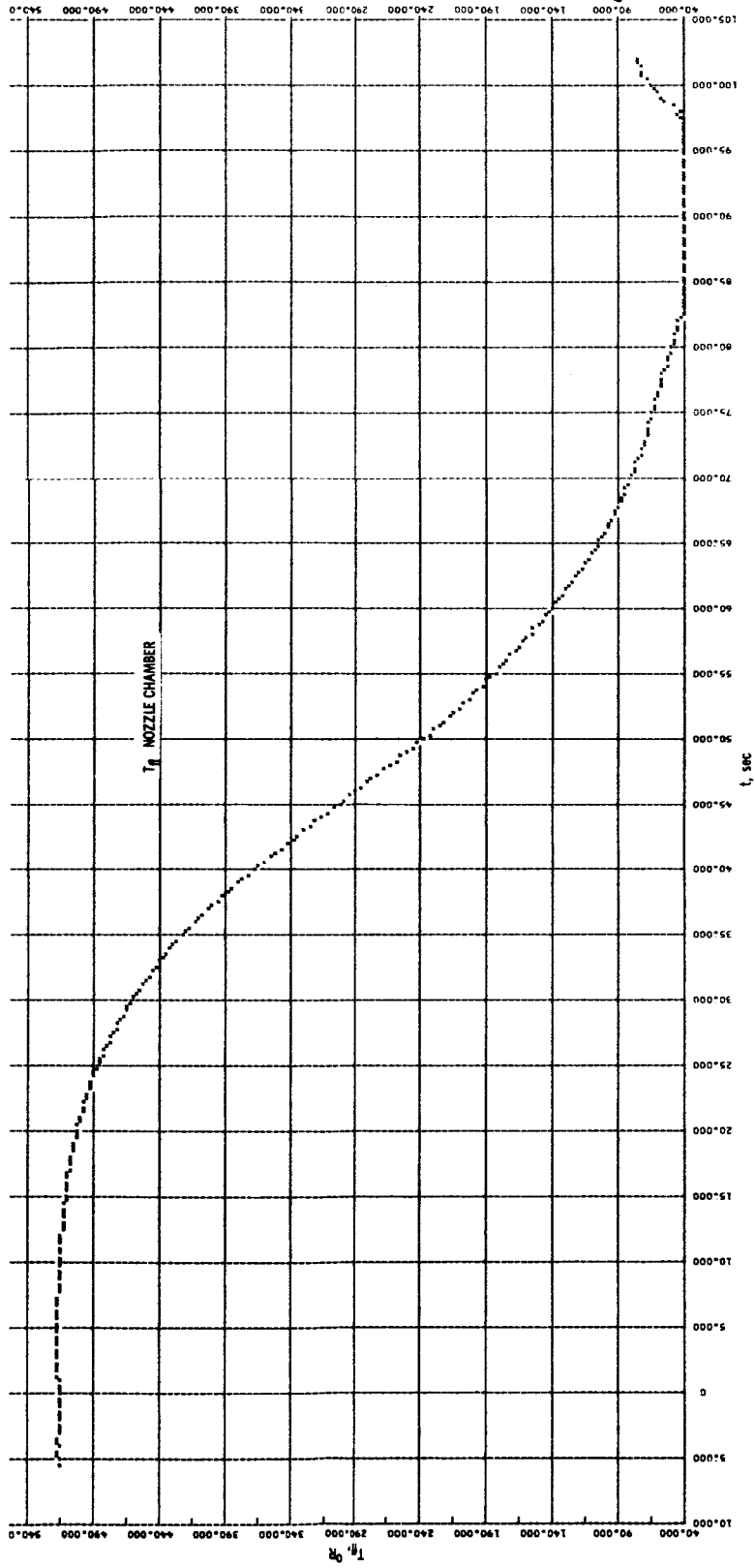


Figure 19. - Nozzle chamber fluid temperature versus time (item no's. NT 60, NT 61, and NT 62).

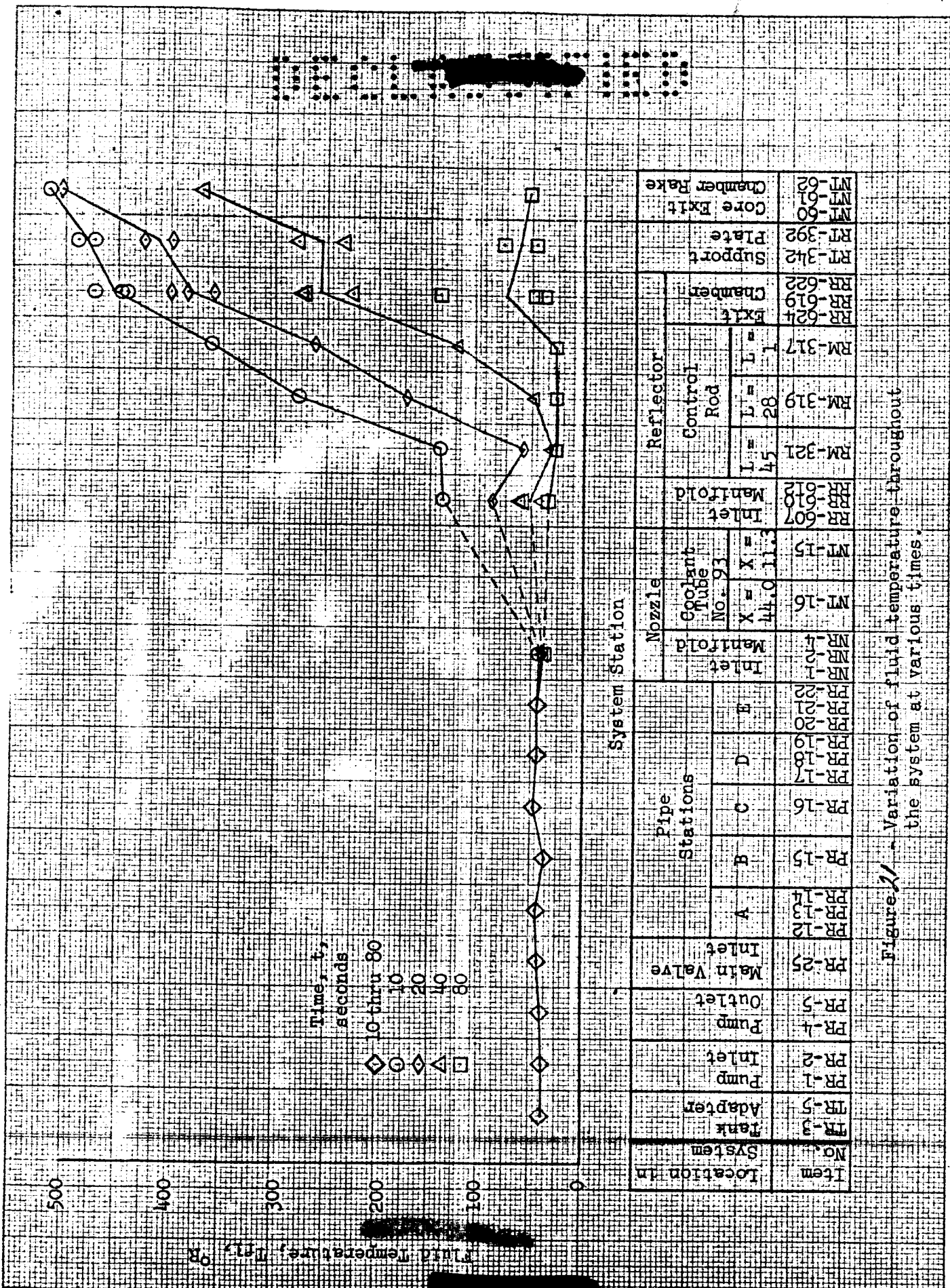


Figure 2 - Variation of fluid temperature throughout the system at various times.

SECRET

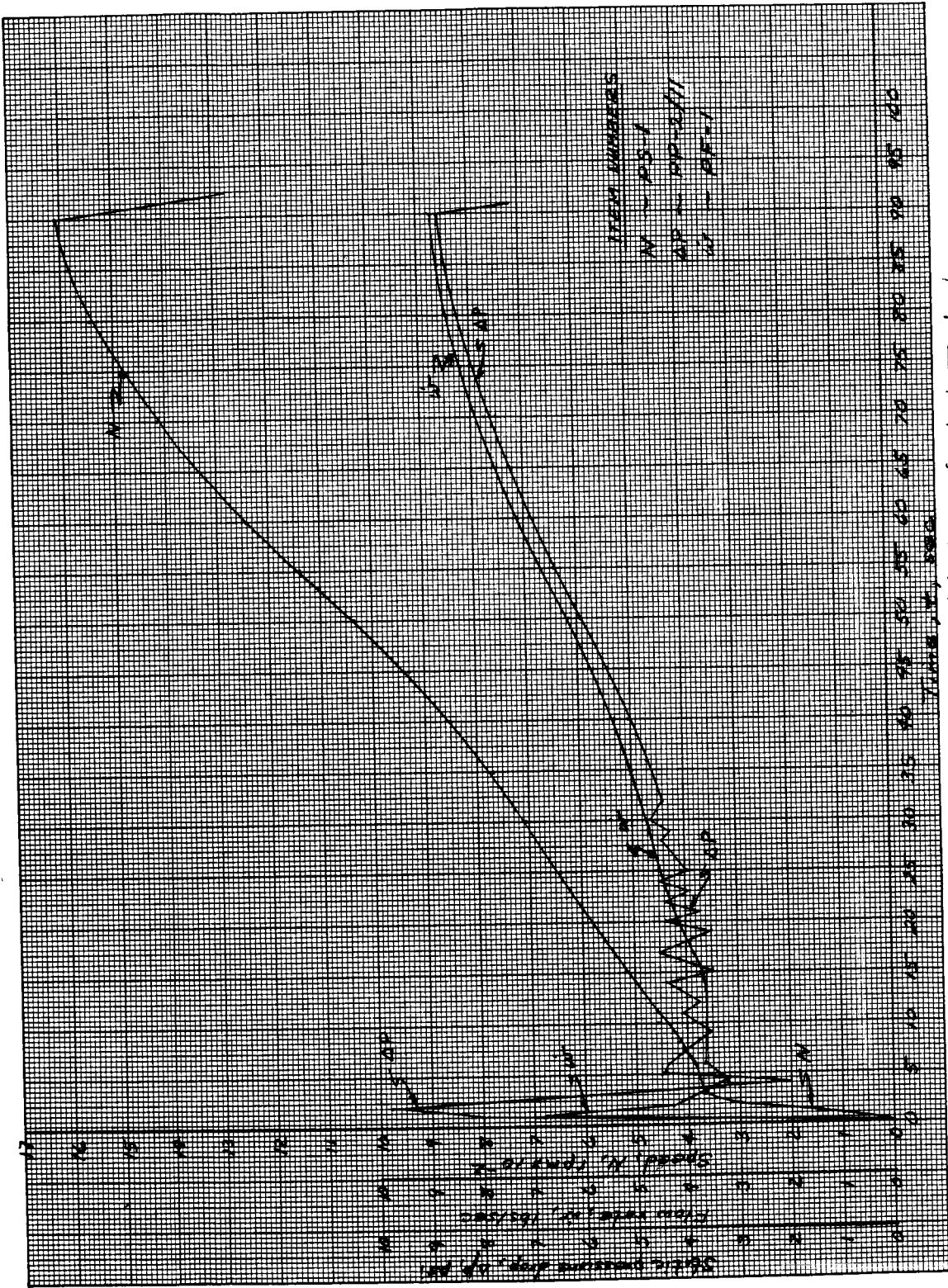


Figure 22 - System start up history of Mark II turbopump

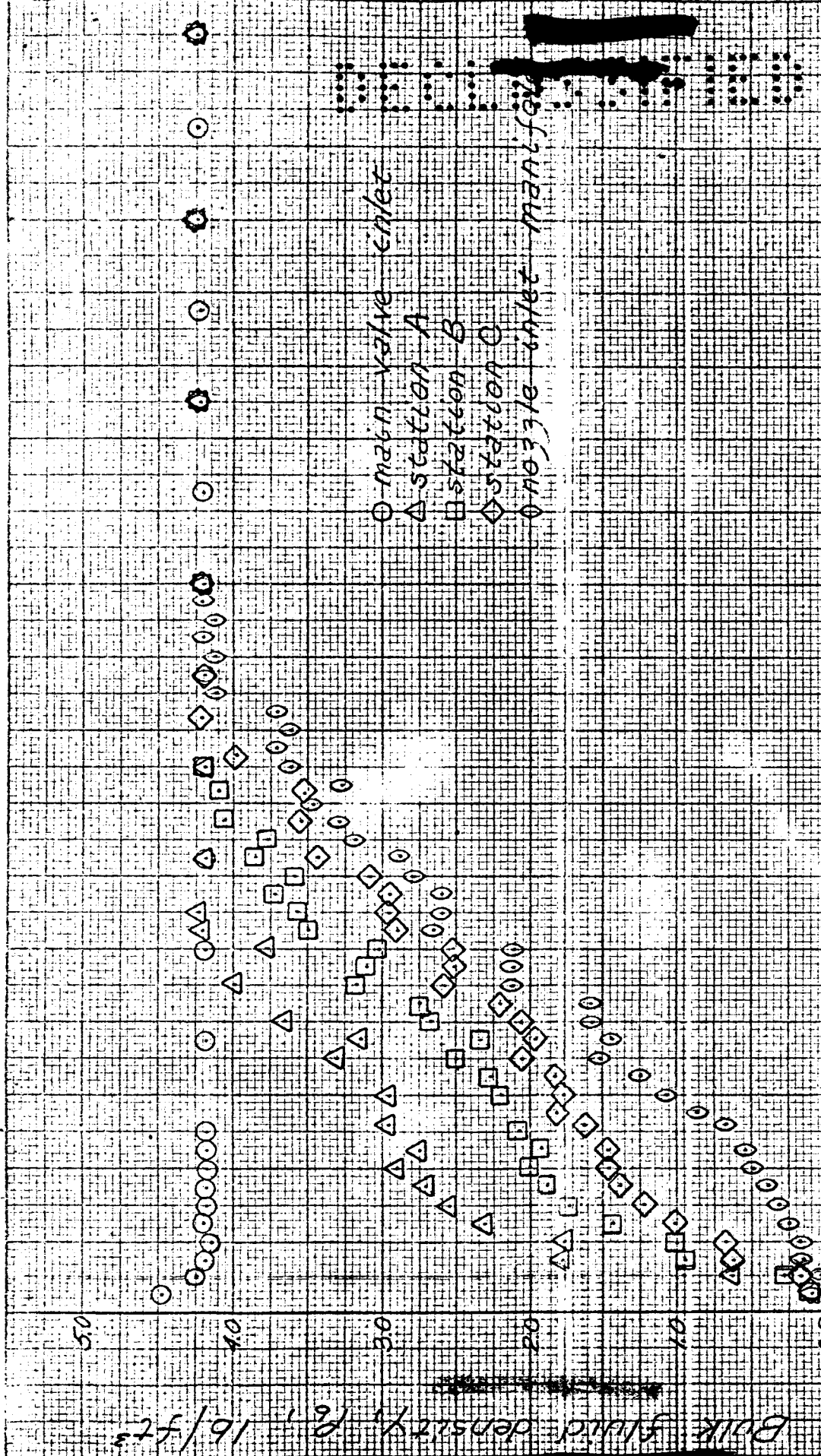


Figure 13. - Variation of bulk fluid density with time at several stations in the feed system piping.

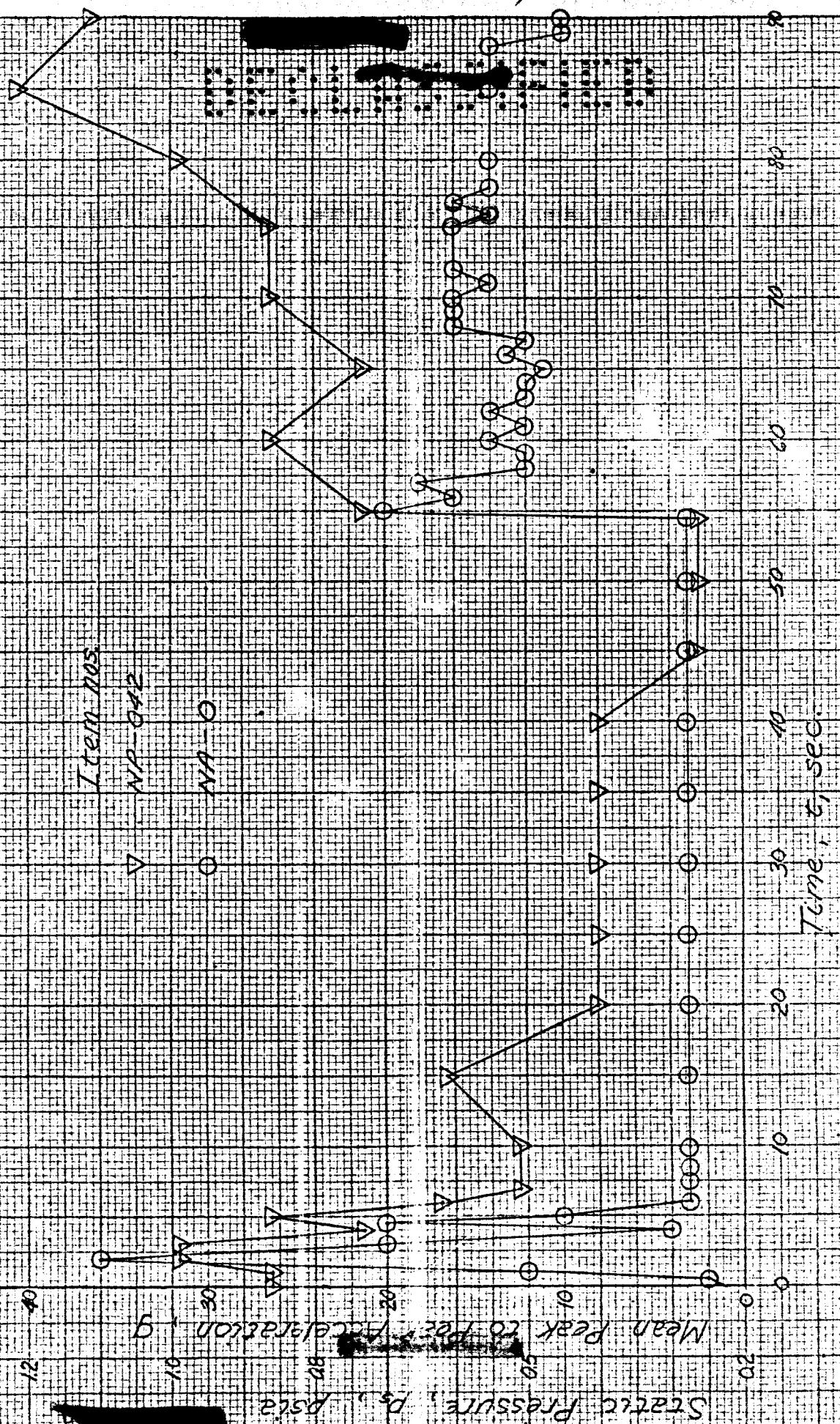


Figure 26 - Time history of static pressure inside nozzle exit bell and vibration g load at nozzle exit

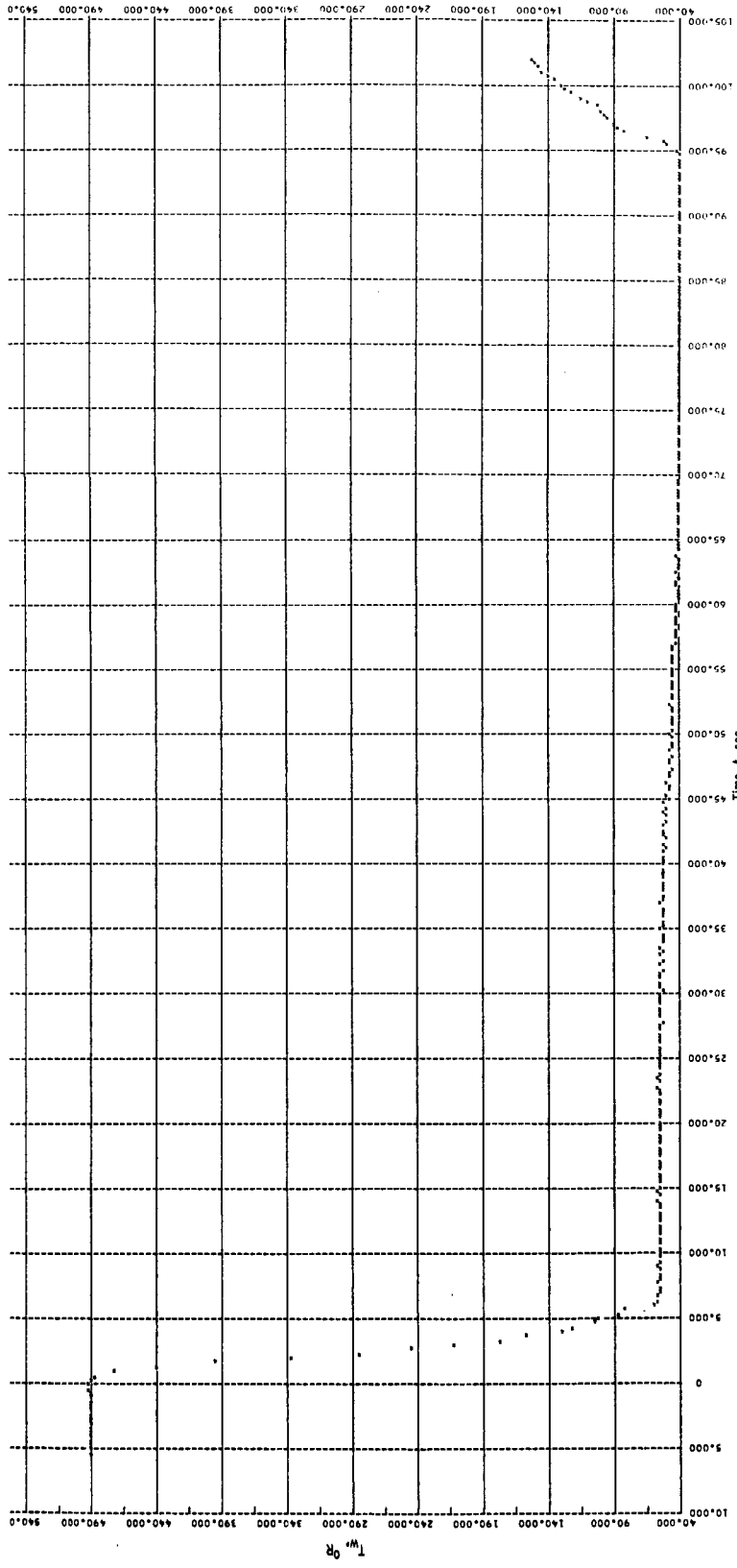


Figure 26. - Nozzle wall temperature versus time on exhaust side (item no. NT 10).

Static pressure difference, ΔP_s , psi

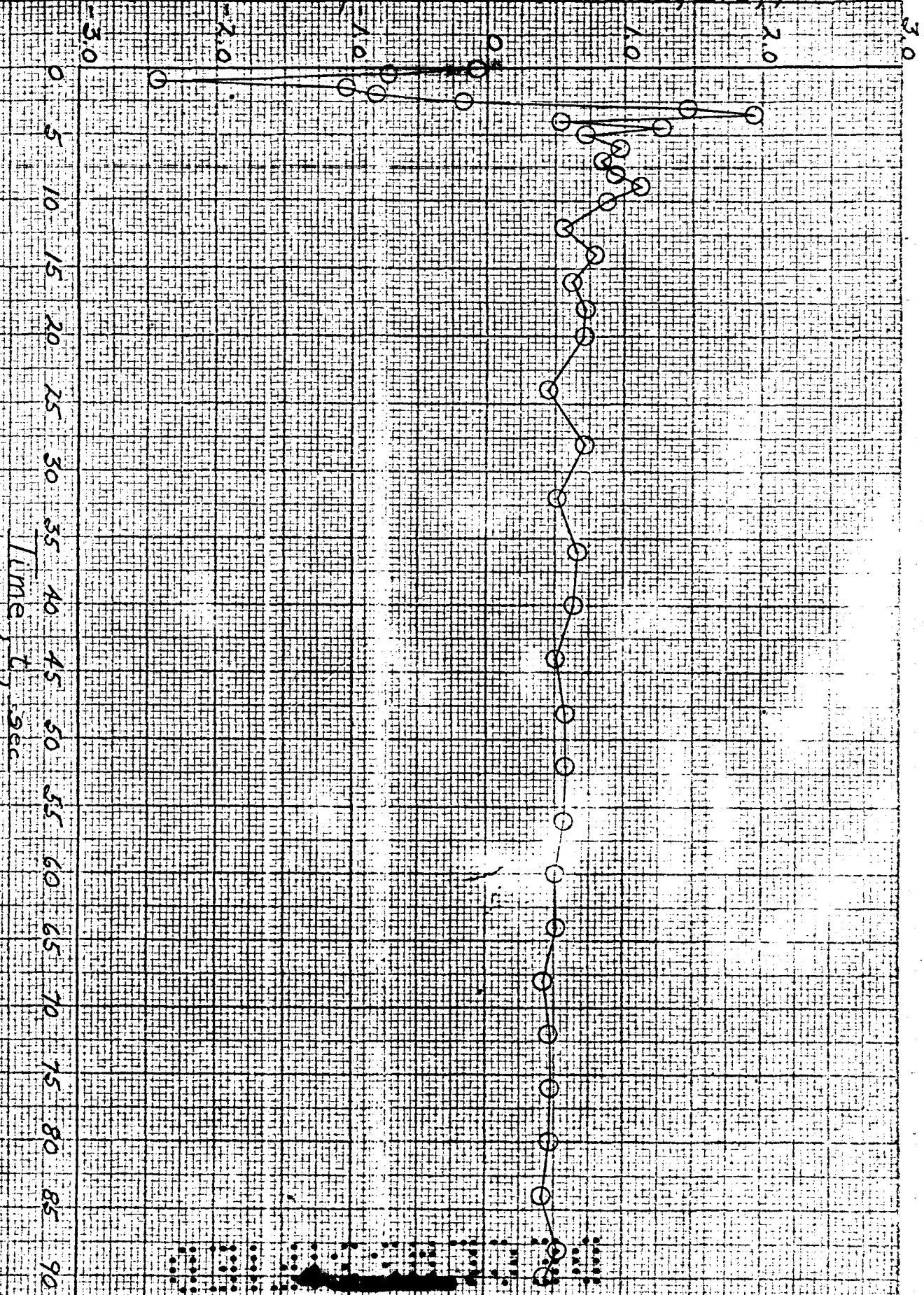
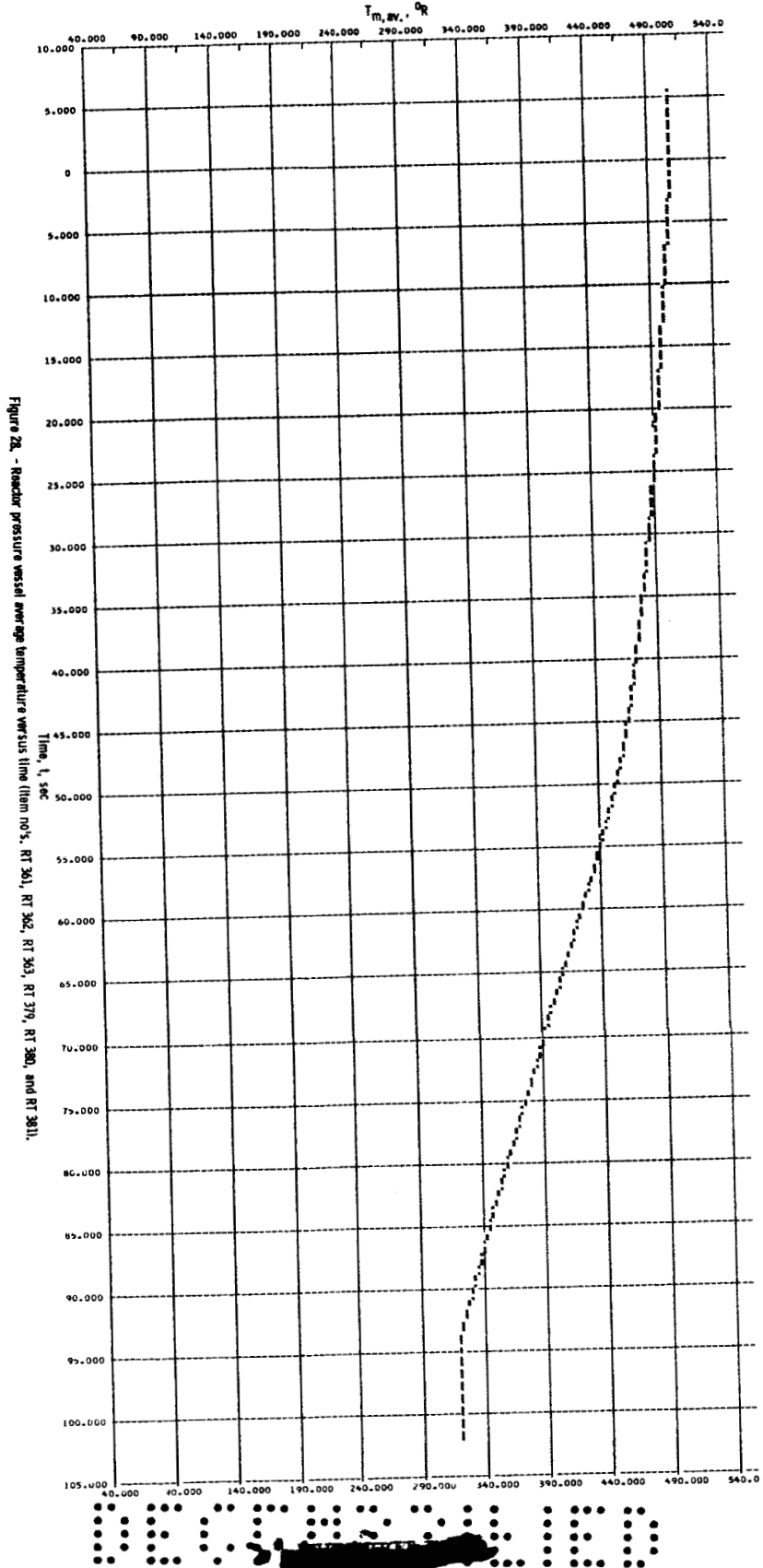


Figure 7: - Static pressure difference between nozzle tube outlet and reflector inlet plenum (Item No. NP-7 minus RP-140)

E-2673



E-2673

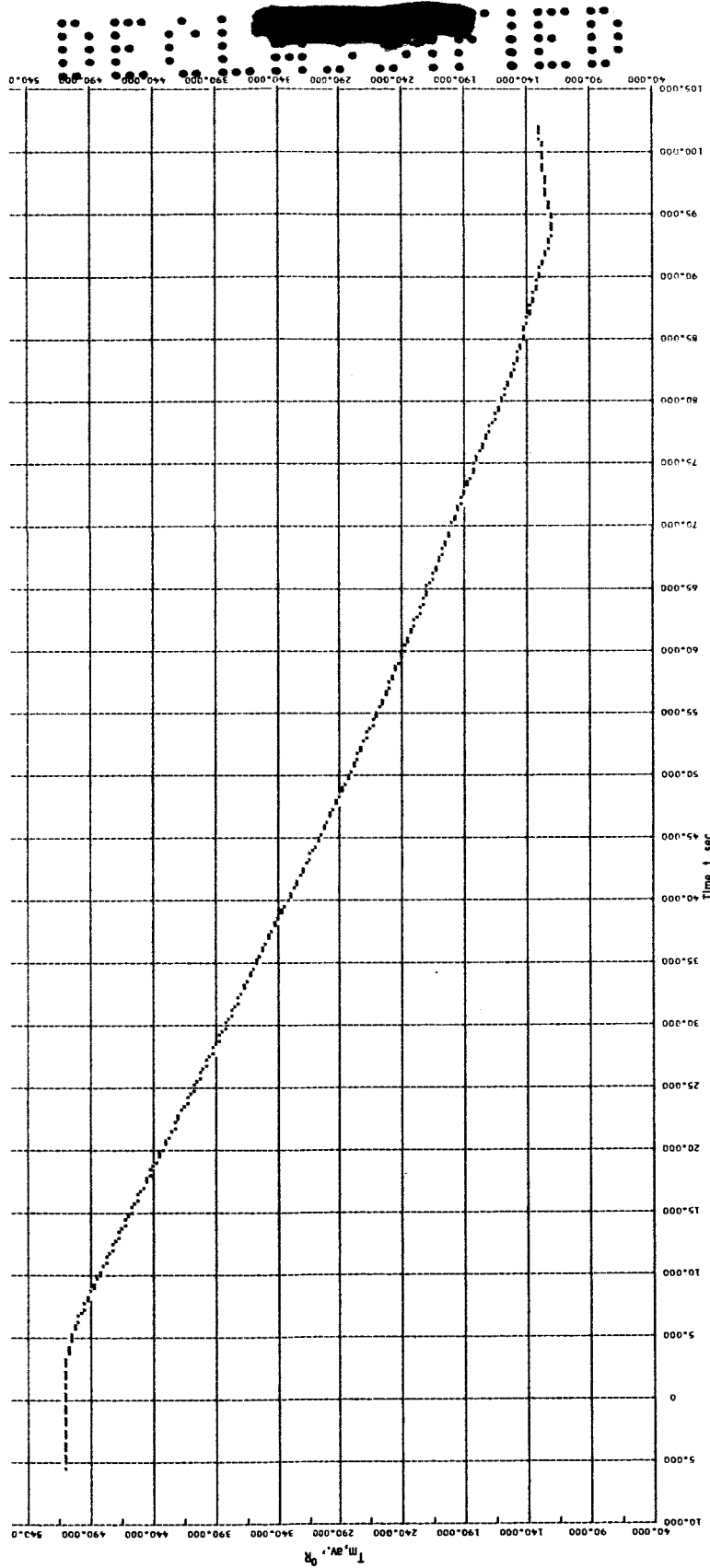


Figure 29. - Main aluminum reflector piece average temperature versus time (Mem no's. RT 170, RT 172, RT 175, RT 176, RT 178, RT 181, RT 182, RT 184, RT 187, RT 188, RT 208, and RT 199).

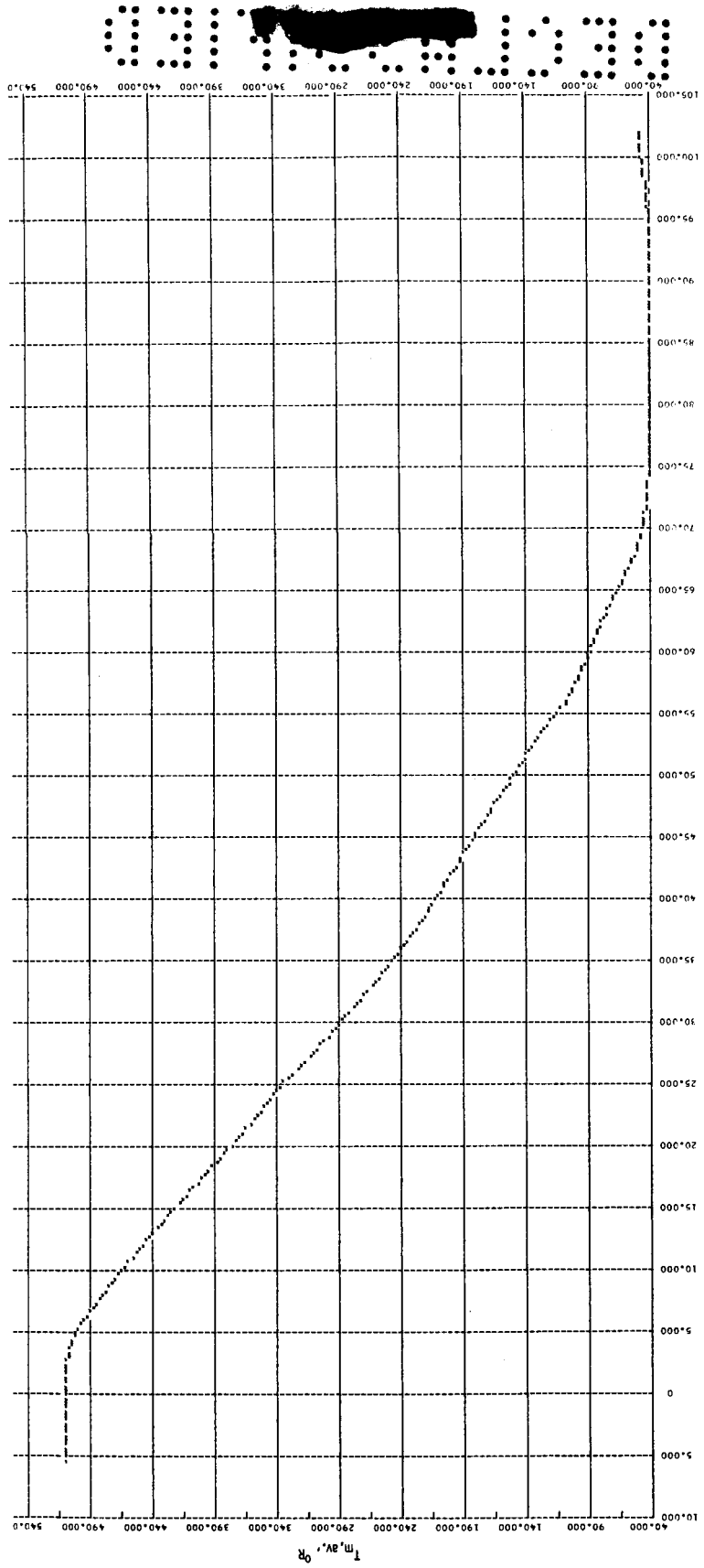


Figure 30. - Average aluminum control rod temperature versus time (item no's. RT 290, RT 291, RT 292, RT 293, RT 294, RT 295, RT 296, RT 297, and RT 298).

E-2673

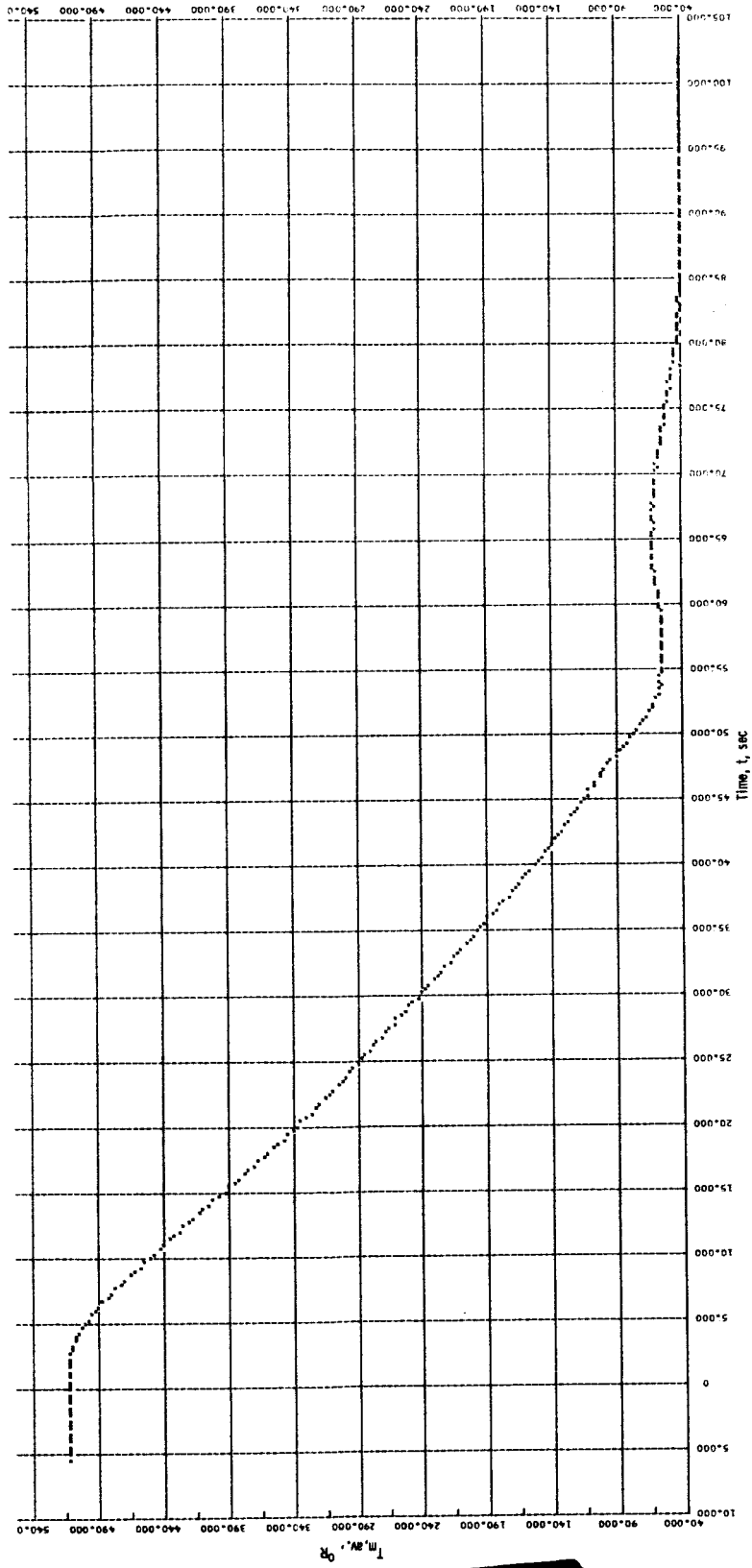


Figure 3L - Average inner graphite reflector cylinder temperature versus time (Item no's. RT 74, RT 75, RT 76, RT 77, RT 78, and RT 79).

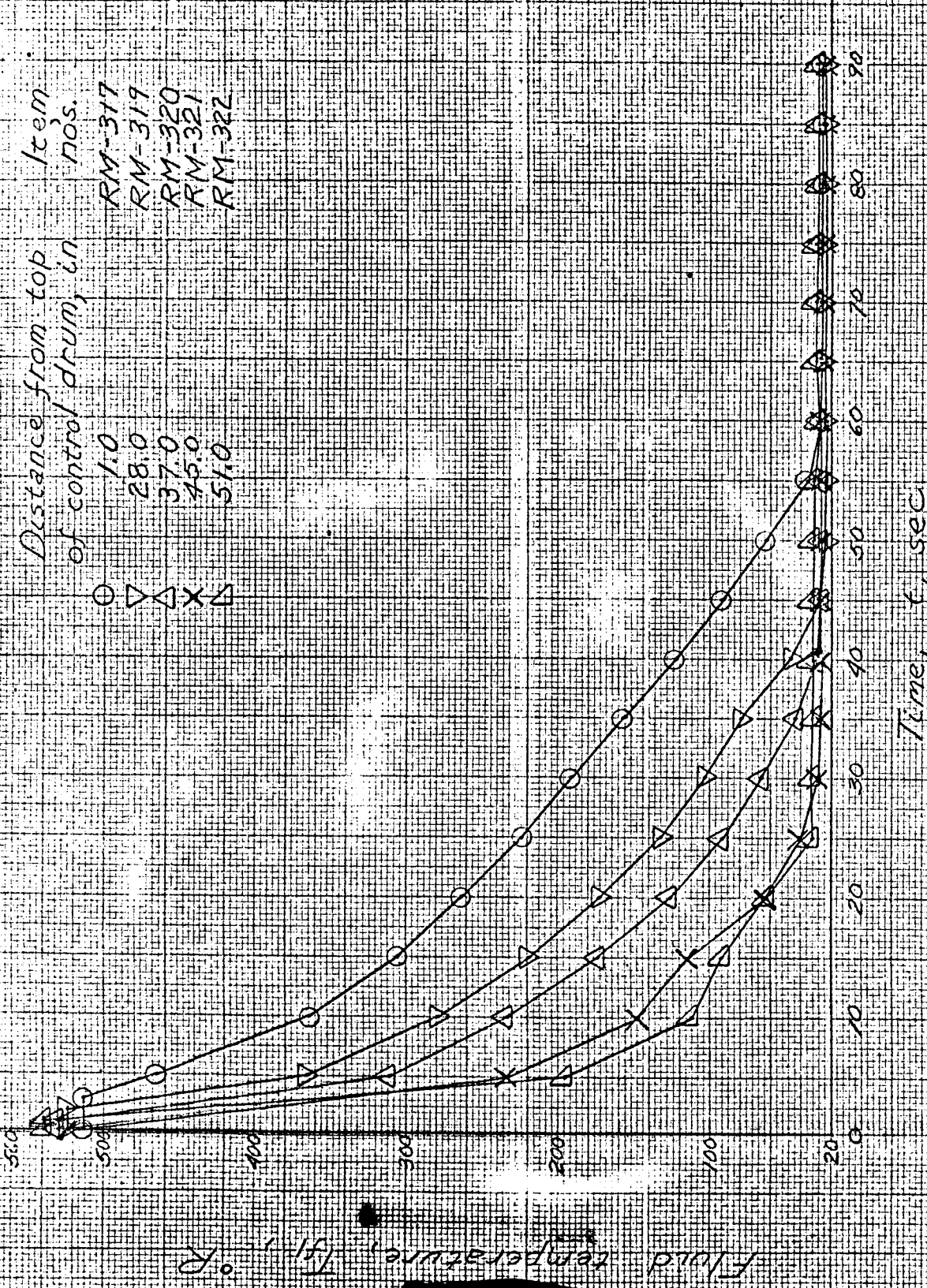


Figure 32 - Variation of fluid temperature with time at five lengthwise stations in the control rod clearance annulus

PRESSURE
VESSEL
WALL

SECRET

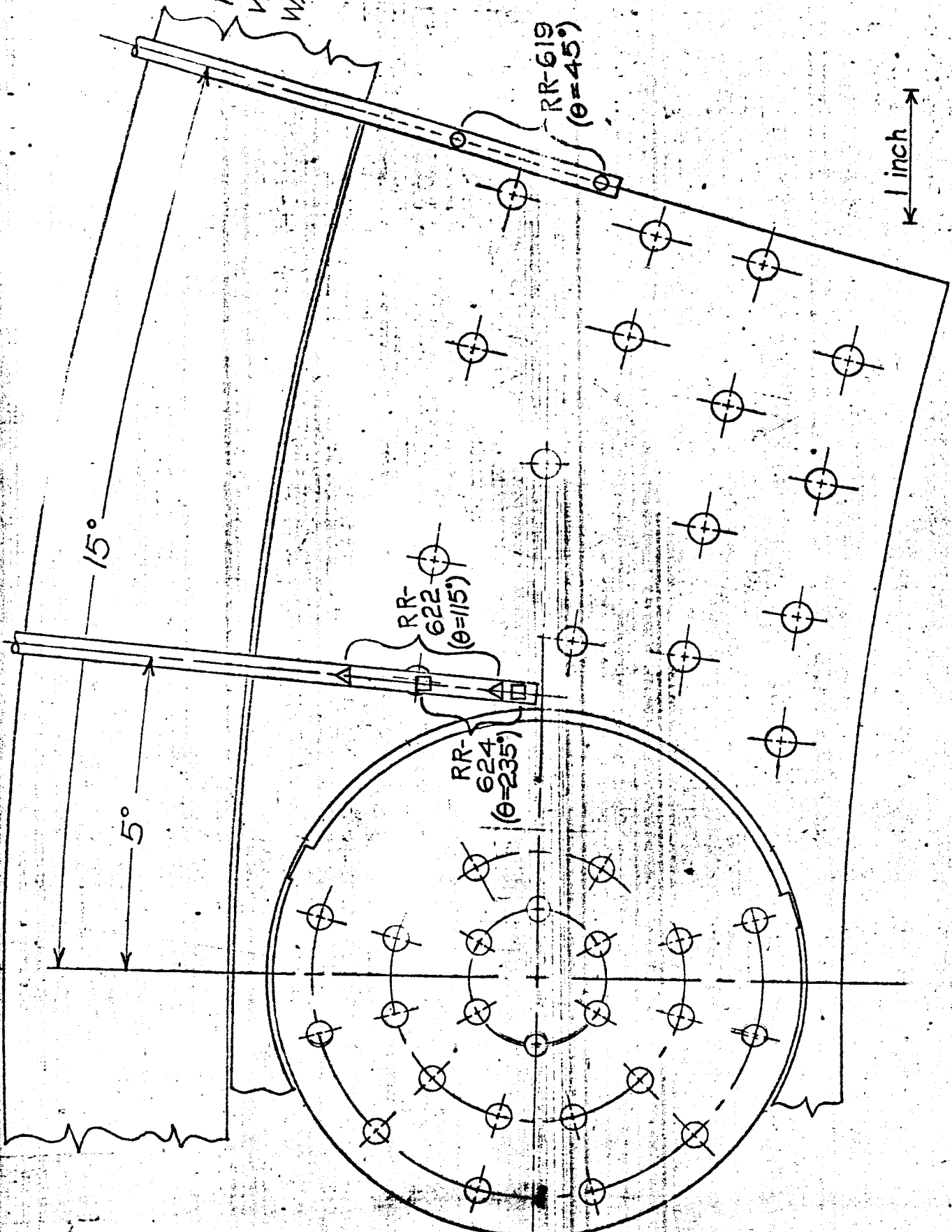


Figure 33 - Reflector outlet sketch showing location of fluid temperature sensors.

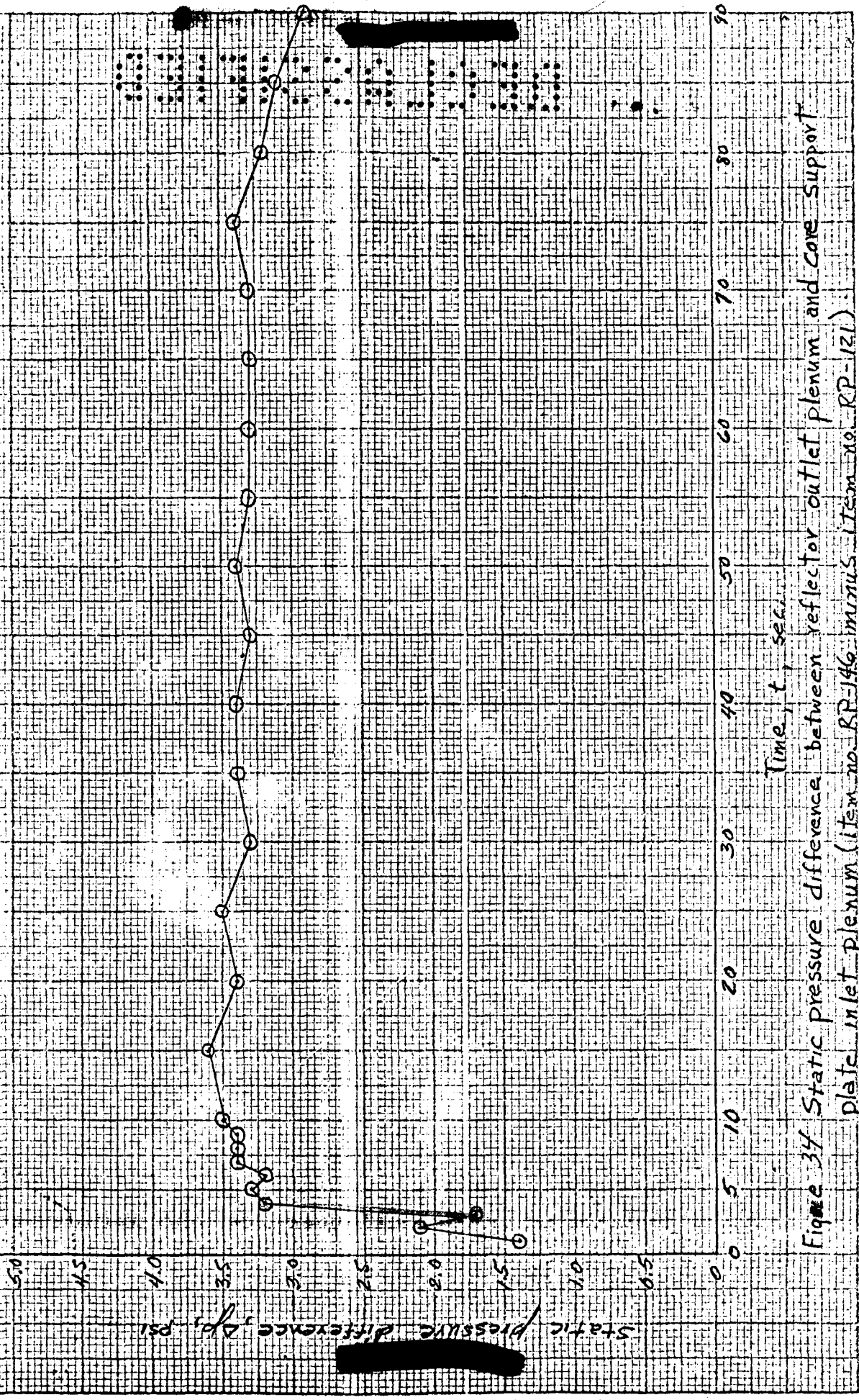


Figure 34 Static pressure difference between reflector outlet plenum and core support plate inlet plenum (item no. RP-146 minus item no. RP-121).

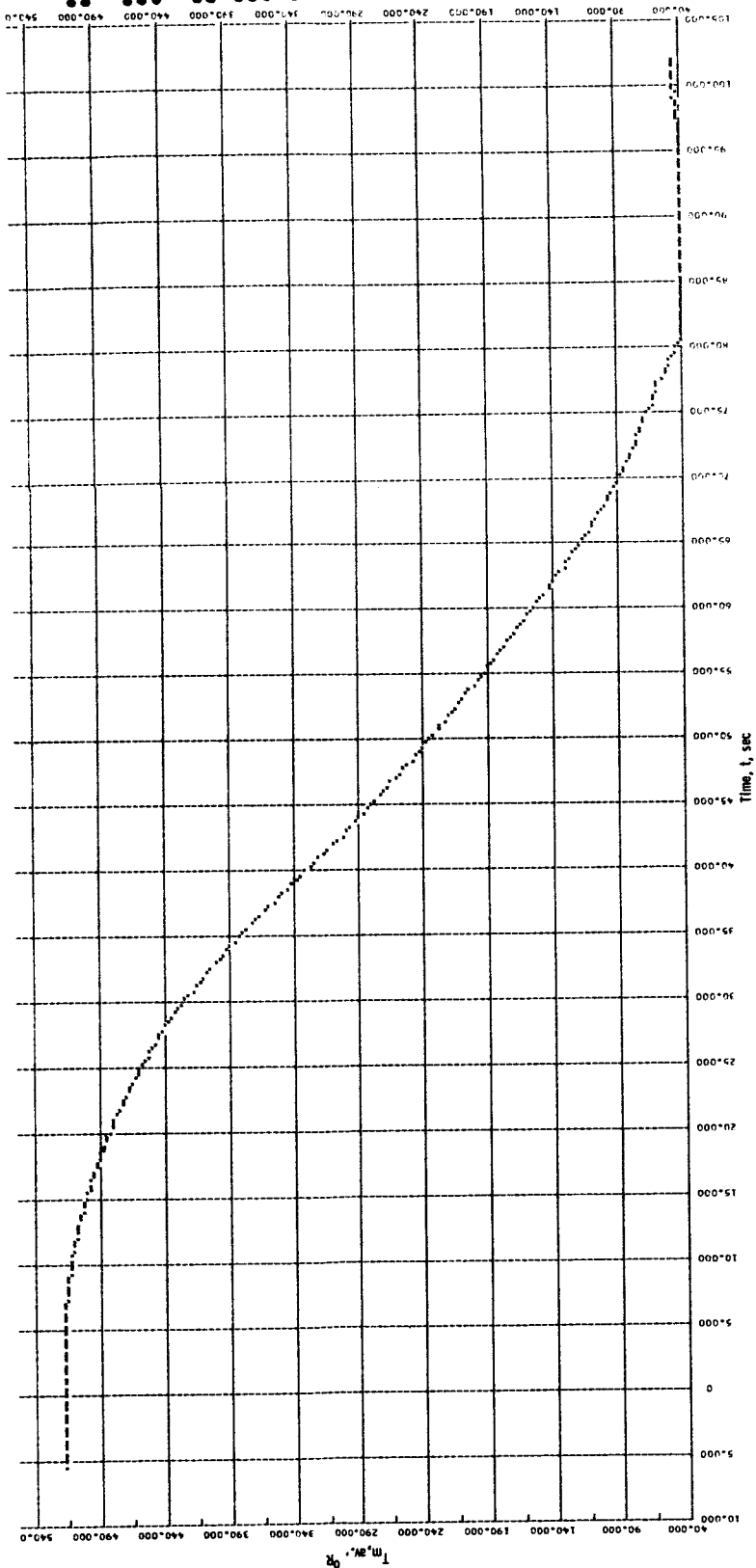


Figure 35. - Average graphite core module temperature versus time for a module at the center of the reactor (item no's. RT 31, RT 32, RT 33, RT 34, and RT 35).

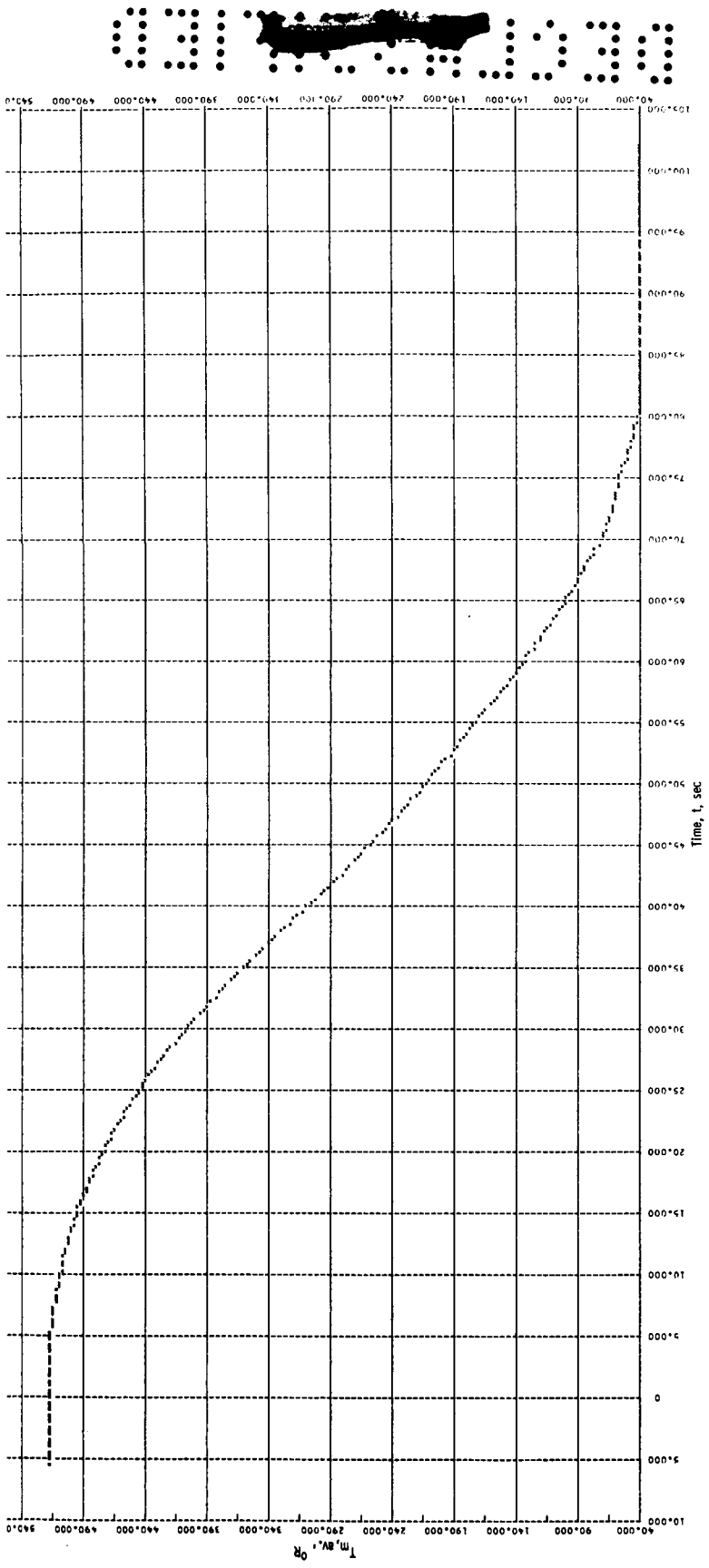


Figure 36. - Average graphite fuel element temperature versus time for a fuel element at the center of the reactor (item no's. RT 1, RT 2, RT 3, RT 4, and RT 5).

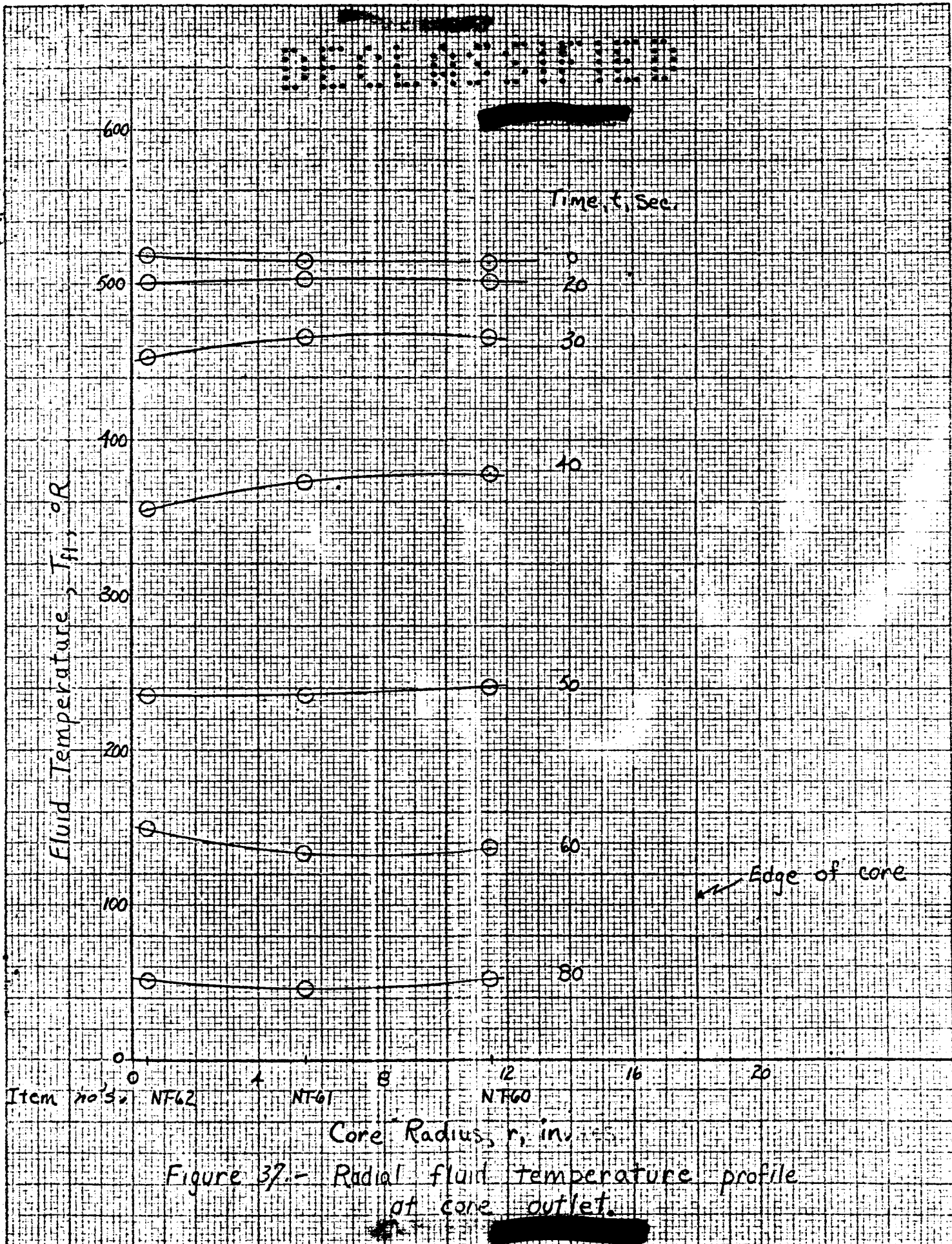


Figure 37.- Radial fluid temperature profile at core outlet.

